END
DATE
FILMED
1 82
DTIQ

LEVEL II (13)

REPORT DOCUMENTATION PAGE		READ INSTRUCTIONS BEFORE COMPLETING FORM
1. REPORT NUMBER Technical Report No. 81-14	2. GOVT ACCESSION NO. AD-A107716	3. RECIPIENT'S CATALOG NUMBER
4. TITLE (and Subtitle) Electron Paramagnetic Resonance Saturation Characteristics of Pristine and Doped Poly-acetylenes.		5. TYPE OF REPORT & PERIOD COVERED Interim. Technical Report
		6. PERFORMING ORG. REPORT NUMBER
7. AUTHOR(s) James C. W. Chien, Gary E. Wnek, Frank E. Karasz, John M. Warakomski, L. Charles Dickinson, A. G. MacDiarmid* and A. J. Heeger⊥		8. CONTRACT OR GRANT NUMBER(s) N00014-81-K-0648
9. PERFORMING ORGANIZATION NAME AND ADDRESS Department of Polymer Science and Engineering University of Massachusetts, Amherst, MA 01003 Department of Chemistry* and Physics⊥ University of Pennsylvania, Philadelphia, PA 19104		10. PROGRAM ELEMENT, PROJECT, TASK AREA & WORK UNIT NUMBERS NR-356-602-4-13-91
11. CONTROLLING OFFICE NAME AND ADDRESS Department of the Navy Office of Naval Research Arlington, VA 22217		12. REPORT DATE November 11, 1981
		13. NUMBER OF PAGES 51
14. MONITORING AGENCY NAME & ADDRESS(if different from Controlling Office)		15. SECURITY CLASS. (of this report) Unclassified
		15a. DECLASSIFICATION/DOWNGRADING SCHEDULE

16. DISTRIBUTION STATEMENT (of this Report)

Distribution unlimited; approved for public release.

17. DISTRIBUTION STATEMENT (of the abstract entered in Block 20, if different from Report)

Accepted for publication in Macromolecules.

DTIC ELECTE NOV 23 1981 D

18. SUPPLEMENTARY NOTES

81 11 20 009

20. ABSTRACT (Continue on reverse side if necessary and identify by block number)

Electron paramagnetic resonance saturation experiments have been carried out on undoped polyacetylene and in the doped polymer as a function of dopant concentration. The relaxation times of undoped trans-$(CH)_x$ show considerable variability from sample to sample, $T_1 = (2.7 \pm 1.7) \times 10^{-5}$ sec and $T_2 = (7.8 \pm 1.0) \times 10^{-8}$ sec suggesting sensitivity to trace impurities. Exposure to air reduces T_1 to 8.1×10^{-6} sec and T_2 to 6.0×10^{-8} sec; this effect is reversible. Using radio-assay techniques with ^{125}I, it was possible to prepare and char-

AD A107716

DTIC FILE COPY

20. acterize samples of known dopant concentration at the level of parts per million (ppm). There are three distinct regimes which characterize the effect of iodine concentration on the EPR characteristics of trans-$(CHI_y)_x$. From $3 \times 10^{-6} < y < 10^{-3}$, T_1 decreases with increasing y, while T_2 is unaffected. The neutral soliton concentration $[S\cdot]$ decrease as $y^{-3.7}$ suggesting that the dopant is predominantly in the material as I_3^- with the remainder as I_5^-. When y exceeds 10^{-3}, there are one or more dopant molecules per $(CH)_x$ chain and the number of neutral solitons is significantly reduced. In the heavily doped samples, the EPR has a Dysonian lineshape until it vanishes for $y > 2 \times 10^{-2}$. The observation of changes in relaxation times even at the dopant level of ppm implies that the dopant ions are randomly distributed throughout the polymer and that the solitons are highly mobile. On the other hand, for cis-$(CH)_x$, doping with iodine from $y = 3.3 \times 10^{-5}$ to 3.9×10^{-4} does not significantly affect T_1 or T_2; for pristine cis-$(CH)_x$, $T_1 = (5.4 \pm 0.9) \times 10^{-5}$ sec and $T_2 = (1.0 \pm 0.07) \times 10^{-8}$ sec. Therefore, the solitons in cis-$(CH)_x$ have low diffusivity. Very slowly doped trans-$[CH(AsF_5)_y]_x$ also displays three characteristic regions. In the dilute regime, T_1, T_2, $[S\cdot]$, and the H_{pp} dependence on H_1 are not significantly different from pristine trans-$(CH)_x$. Above $y > 6 \times 10^{-3}$, $[S\cdot]$ first decreases with y, then the EPR intensity increases rapidly as the Pauli susceptibility makes its contribution. In the transitional regime, $6 \times 10^{-3} < y < 5 \times 10^{-2}$, the resonance could not be saturated with the power available implying anomalously short relaxation times (T_1), whereas saturation was again possible in the heavily doped metallic limit.

Electron Paramagnetic Resonance Saturation Characteristics
of Pristine and Doped Polyacetylenes

by

James C. W. Chien, Gary E. Wnek, Frank E. Karasz,
John M. Warakomski, L. Charles Dickinson,
Alan G. MacDiarmid* and Alan J. Heeger[†]

Department of Polymer Science and Engineering
University of Massachusetts
Amherst, MA   01003
Departments of Chemistry* and Physics[†]
University of Pennsylvania
Philadelphia, PA   19104

November 11, 1981

Electron Paramagnetic Resonance Saturation Characteristics

of Pristine and Doped Polyacetylenes[1]

James C.W. Chien*, Gary E. Wnek[2], Frank E. Karasz,

John M. Warakomski and L. Charles Dickinson

Materials Research Laboratory, Department of Polymer Science and Engineering,
Department of Chemistry, University of Massachusetts, Amherst, MA 01003

Alan J. Heeger and Alan G. MacDiarmid

Laboratory for Research on the Structure of Matter, University of Pennsylvania,
Philadelphia, PA 19104

ABSTRACT

Electron paramagnetic resonance saturation experiments have been carried out on undoped polyacetylene and in the doped polymer as a function of dopant concentration. The relaxation times of undoped trans-$(CH)_x$ show considerable variability from sample to sample, $T_1 = (2.7 \pm 1.7) \times 10^{-5}$ sec and $T_2 = (7.8 \pm 1.0) \times 10^{-8}$ sec suggesting sensitivity to trace impurities. Exposure to air reduces T_1 to 8.1×10^{-6} sec and T_2 to 6.6×10^{-8} sec; this effect is reversible. Using radio-assay techniques with ^{125}I, it was possible to prepare and characterize samples of known dopant concentration at the level of parts per million (ppm). There are three distinct regimes which characterize the effect of iodine concentration on the EPR characteristics of trans-$(CHI_y)_x$. From $3 \times 10^{-6} < y < 10^{-3}$, T_1 decreases with increasing y, while T_2 is unaffected. The neutral soliton concentration $[S\cdot]$ remains constant in this region. Dilute doping results in conversion of $S\cdot$ to a spinless positive soliton S^+ and/or direct oxidation of $(CH)_x$ to create S^+S^+ pairs. In the intermediate concentration regime, $10^{-3} < y < 10^{-2}$, both T_1 and T_2 decrease with y, and $[S\cdot]$ decrease as $y^{-3.7}$ suggesting that the dopant is predominantly in the material as I_3^- with the remainder as I_5^-. When y exceeds 10^{-3}, there are one or more dopant molecules per $(CH)_x$ chain and the number of neutral solitons is significantly reduced. In the heavily doped samples, the EPR has a Dysonian lineshape until it vanishes for $y > 2 \times 10^{-2}$. The observation of changes in relaxation times even at the dopant level of ppm imples that the dopant ions are randomly distributed throughout the polymer and that the solitons are highly mobile. On the other hand, for cis-$(CH)_x$, doping with iodine from $y = 3.3 \times 10^{-5}$ to 3.9×10^{-4} does not significantly affect T_1 or T_2; for pristine cis-$(CH)_x$, $T_1 = (5.4 \pm 0.9) \times 10^{-5}$ sec

and $T_2 = (1.0 \pm 0.07) \times 10^{-8}$ sec. Therefore, the solitons in cis-$(CH)_x$ have low diffusivity. Very slowly doped trans-$[CH(AsF_5)_y]_x$ also displays three characteristic regions. In the dilute regime, T_1, T_2, [S·], and the ΔH_{pp} dependence on H_1 are not significantly different from pristine trans-$(CH)_x$. Above $y > 6 \times 10^{-3}$, [S·] first decreases with y, then the EPR intensity increases rapidly as the Pauli susceptibility makes its contribution. In the transitional regime, $6 \times 10^{-3} < y < 5 \times 10^{-2}$, the resonance could not be saturated with the power available implying anomalously short relaxation times (T_1), whereas saturation was again possible in the heavily doped metallic limit.

INTRODUCTION

Poly(trans-acetylene), trans-$(CH)_x$, has generated considerable interest among condensed matter physicists because it undergoes a commensurate Peierls distortion (index of 2), to a bond-alternated semiconducting state[3]. Upon injection of an electron-hole pair, or upon doping to form either electron pairs or hole pairs, the lattice is unstable to the formation of charged solitons[4,5]. Results of the magnetic[6,7], electric[8,9], spectroscopic[10-12], and doping properties[13] of trans-$(CH)_x$ support the soliton hypothesis[4,5,13]. Electron paramagnetic resonance (EPR) studies[14-16] of neutral defects in undoped polymer are also consistent with the concept of solitons[4,5,13]. Moreover, the decrease in Curie-law spin content upon doping is understood in the context of soliton doping, since charged solitons have spin zero.

Recently, the crystal structures of both trans-$(CH)_x$[17] and cis-$(CH)_x$[18] have been determined with electron diffraction. The c-axis is found to be the molecular chain axis and lies parallel to the fiber axis. There is more overlap of π-orbitals between the chains in the unit cell of the trans polymer than between those in the cis material, suggesting possible smaller interchain resistance to charge carrier transport. The results on trans-$(CH)_x$ has been confirmed by a recent x-ray diffraction study on oriented specimens[19].

There has not been a systematic investigation of EPR saturation characteristics on these polymers. This has now been performed for pristine and doped cis and trans polyacetylenes with special emphasis in the low doping levels; the

results are reported here. The results of these investigations shed light on questions concerning the homogeneity of dopant, the mobility of the solitons and the mechanism of doping.

EXPERIMENTAL SECTION

A. Preparation of polyacetylenes.

Acetylene was polymerized using the $Ti(O-n-C_4H_9)_4-AlEt_3$ catalyst as previously described[20-23]. The nascent morphology of $(CH)_x$ is comprised of fibrils ca. 200 Å in diameter as shown by the early studies of Ito et al.[21] and more recently for thin films polymerized directly on an electron microscope grid[24]. Films of cis-$(CH)_x$ were also prepared according to standard techniques[20-23] and stored in vacuo at -78°C until use. Typical analysis of the material is: C, 91.26%; H, 7.92%; total, 99.18%; calculated for $(CH)_x$: C, 92.26%; H, 7.74%. The cis-$(CH)_x$ samples used in this study had a cis-content in the range 85-88% as determined by its absorption intensities[20]. For trans-$(CH)_x$, the samples were immediately isomerized by heating at 200°C for 2 hours in vacuo. The polymers were never exposed to air; the dry box used for their transfer contains <2 ppm O_2. Perdeuterated polyacetylene was obtained with C_2D_2 prepared from CaC_2 reaction with 99.8% D_2O.

B. Doping.

Iodine doping was carried out in an apparatus where a film of $(CH)_x$ was mounted on a probe with four electrical leads. Several additional films were also contained in the vessel. The vessel was connected via a teflon stopcock to an iodine reservoir maintained at a partial pressure of 3×10^{-3} torr. The entire assembly can be connected to a standard vacuum line. The polymer was doped to

desired conductivity by monitoring the resistance of the film mounted on the four-probe. The other specimens were used in various physical and chemical investigations. The amount of iodine in heavily doped polymer was determined by weight gain. Overlapping with the former, but extending far into lower doping levels, we used $^{125}I_2$ and determined its concentration in the polymer by radio-assay. The counting efficiency was found to be 55.3%.

Even at these very dilute levels, the conductivity was sensitive to the dopant concentration, ($\underline{y}$); the carrier concentration increases slowly but steadily with doping. The increase in conductivity with $\underline{y}$ for iodine at the ppm level (obtained with the four-probe technique) is shown in Figure 1.

Figure 1

A very slow doping procedure was developed for AsF_5, as described in detail elsewhere[25], and was used in this study. In certain cases, it was of interest to dope polyacetylene to very low levels directly in an EPR tube (referred to as in situ doping). Extremely small quantities of gas were metered as follows. With the AsF_5 bulb cold finger cooled to -95°C and the stopcock between the bulb and manifold closed, the stopcock of the bulb was opened briefly, allowing AsF_5 (ca. 30 torr at -95°C) to fill this small volume. The bulb was then closed, the gas was expanded into the manifold and the stopcock isolating the bulb and the manifold was closed. The AsF_5 in the manifold was pumped away and the very small portion of AsF_5 remaining between the bulb and manifold was then allowed to contact the film in the EPR tube. The tube was then disconnected from the vacuum line and a spectrum was recorded. A few such consecutive dopings were sometimes required to yield the desired results.

3. EPR measurements.

A Varian E-9 X-band spectrineter was used in the EPR studies. Most measurements are expressed in terms of the input power from the kystron. To obtain spin-lattice relaxation times, the actual microwave power in the TE_{102} cavity, H_1, was needed. This was obtained by the method of a perturbing sphere[26]. A metal sphere was placed in the EPR cavity and the shift in frequency $\Delta\nu$ was measured as a function of klystron power W (watts). The H_1 in gauss was then calculated from

$$|H_1| = \tfrac{1}{2}\left[W\left(\frac{\nu^2 - \nu_0^2}{\nu_0^2}\right)\left(\frac{40}{\pi^2 \Delta\nu a^3}\right)\right]^{1/2} \tag{1}$$

where W is klystron power in watts, $\nu_0 = 9.545$ GHz and $\nu = 9.554 \times 10^9$ GHz are the initial and perturbed frequencies, and a is the radius of the sphere = 1.59 mm. We found the relationship

$$|H_1|^2 = 0.49\ W \tag{2}$$

Saturation curves were obtained by recording EPR spectra as a function of microwave power at 2-5 mW increments up to 200 mW which is the maximum power available from the klystron. From the plot of signal amplitude versus W, $H_{1\underline{m}}$ is found for maximum signal amplitude. Together with $\Delta H_{\underline{pp}}$ below saturation, the spin-lattice and spin-spin relaxation time (T_1 and T_2, respectively) were

calculated[27]

$$T_1 = 1.97 \times 10^{-7} \; \Delta H_{pp} \; [\underline{g} \; (H_1,\underline{m})^2]^{-1} \; sec \qquad (3)$$

and

$$T_2 = 1.313 \times 10^{-7} \; [\underline{g} \; \Delta H_{pp}]^{-1} \; sec \qquad (4)$$

Since relatively high microwave powers were employed, the possibility of sample heating and associated distortion of the saturation curves was investigated. The temperatures of a series of samples of $\underline{cis}$-$[CH(AsF_5)_{\underline{y}}]_{\underline{x}}$ were measured directly with a thermocouple attached to the sample with Electrodag, while simultaneously carrying out saturation measurements. Since the conducting Electrodag could be expected to heat at high microwave power, the measured temperature should provide a reliable upper limit of the sample temperature in the absence of the thermocouple. As indicated in Figure 2, the sample temperature increased linearly with power and the slope increased with $\underline{y}$. In all samples with $\underline{y} > 1.8 \times 10^{-2}$, the sample tube was noticeably warm to the touch after completion of the saturation experiment. Similar effects were observed for $\underline{cis}$-$(CHI_{\underline{y}})_{\underline{x}}$ doped to fairly high levels ($\underline{y} > 0.02$); the sample tubes were also noticeably warm upon completion of the saturation measurements though the actual sample temperatures were not monitored. Furthermore, doped $\underline{trans}$-$(CH)_x$ samples also display microwave heating. The heating was an off-resonance phenomenon; maintaining the magnetic field several hundred gauss off resonance yielded the same temperature as obtained when scanning through resonance. The attached

Figure 2

thermocouple did not affect ΔH_{pp}, the A/B ratio of Dysonian lines, or the saturation behavior, as similar samples without a thermocouple yielded similar results. Thus, although sample heating was detected, such effects are not important at dilute doping levels (i.e. below $y=0.02$). The experimental results, presented in the next section, were obtained using samples with no thermocouple.

RESULTS

A. Undoped trans-(CH)$_x$ and cis-(CH)$_x$.

The EPR saturation curve for undoped trans-(CH)$_x$ approaches the case of homogeneous broadening (Figure 3). The signal, Y_m, is of the form

$$Y_m = z/(1 + z^2) \qquad (5)$$

where $z = \gamma H_1(T_1 T_2)^{1/2}$. Measurements were made on samples from many preparations. At ambient temperatures, the values of T_1 range from 1.9 to 6.6 x 10^{-5} sec with an average value of (2.7 ±1.7) x 10^{-5} sec. The values of T_2 range from 6 to 8.8 x 10^{-8} sec with an average value of (7.8 ±1.0) x 10^{-8} sec. Therefore, the variability in T_1 is much greater than it is for T_2 in trans-(CH)$_x$. At 77°K, T_1 was increased to 6.8 x 10^{-5} sec while T_2 was reduced to 2.2 x 10^{-8} sec.

The effect of oxygen is also shown in Figure 3. In this experiment, undoped trans-(CH)$_x$ was exposed to air for 30 min at ambient temperature. The EPR of the neutral soliton becomes inhomogeneously broadened with values of $T_1 = 8.1$ x 10^{-6} sec and $T_2 = 6.6$ x 10^{-8} sec. Evacuation of the sample overnight at 10^{-6} torr restored the EPR saturation characteristics to that of the original material. Therefore, under these conditions, the effect of oxygen is reversible. Qualitatively similar effects on the linewidth (T_2) were reported earlier by Goldberg et al.[14]

Saturation measurements were carried out, in addition, on many cis-(CH)$_x$ preparations. A few typical curves are shown in Figure 4. The values of T_1 for

seven samples are 49, 39, 63, 47, 63 and 58 μsec giving an average value of
$(5.3 \pm 0.9) \times 10^{-5}$ sec. The values for T_2 are 10, 10, 10, 9, 9.4, 11 and 11 nsec
for an average of $(1.0 \pm 0.07) \times 10^{-8}$ sec. Figure 4 also shows the saturation
curve for undoped $(CD)_x$ giving $T_1 \approx 4 \times 10^{-6}$ sec and $T_2 = 1.2 \times 10^{-8}$ sec.

B. Iodine doped trans-$(CH)_x$.

Several saturation curves of iodine doped trans-$(CHI_y)_x$ obtained at ambient
Figure 5 temperature are shown in Figure 5 to indicate the trend. Doping in the range of
y from 3×10^{-6} to 3×10^{-3} utilized $^{125}I_2$; ordinary iodine was used for $y \geq 7 \times 10^{-4}$.
Therefore, the two methods of determining dopant concentration overlap between
$y = 7 \times 10^{-4}$ and 3×10^{-3}; the results in these regions are in good agreement.
The EPR of trans-$(CHI_y)_x$ generally retains the Lorentzian line shape with some
broadening in the wings. The linewidth does not change with microwave power.
In contrast, the EPR linewidth of undoped trans-$(CH)_x$ increases rapidly with
Figure 6 increasing H_1 (Figure 6). Near the semiconductor metal transition, the EPR
signal assumes a Dysonian line shape; the A/B ratio is 1.0, 1.2 and 1.5 for
$y = 7.5 \times 10^{-4}$, 1.5×10^{-2} and 2.2×10^{-2}, respectively. Figure 5 also shows that
trans-$(CHI_y)_x$ saturation curves do not deviate significantly from homogeneous
broadening even for heavily doped samples.

The saturation curves of trans-$(CHI_y)_x$ at 77°K are qualitatively different
Figure 7 from those at room temperature (Figure 7). At high levels of doping, the low
temperature EPR saturates more slowly, and the signal does not decrease at high
power levels. This may indicate inhomogeneous broadening or may result from a
non-uniform microwave field in the sample due to the skin effect.

The most interesting finding is the very pronounced effect of extremely dilute concentrations of iodine on the relaxation times of doped trans-$(CH)_x$. Iodine is known[28] to exist primarily as I_3^- in doped $(CH)_x$ with some I_5^- present as well. therefore, at our most dilute doping level of 3×10^{-6}, the actual dopant concentration is about 1×10^{-6} for $[(CHI_3)_y]_x$ or even 6×10^{-7} for $[(CHI_5)_y]_x$ (vide infra). Although the linewidth (T_2) is virtually constant throughout the most dilute regime (Figure 8), iodine doping has a significant effect on T_1 even at the levels of a few parts per million. The spin-lattice relaxation time decreases rapidly with increasing y in the lightly doped regime (Figure 9). Above $y > 10^{-3}$ the decrease in T_1 becomes more gradual with further increases in y while T_2 begins to decrease rapidly. The EPR remains saturatable throughout the dilute and intermediate doping levles. The microwave power needed for saturation is, however, a strong function of y (Figure 10).

Figure 8

Figure 9

Figure 10

Examination of the integrated intensity in the EPR line shcws that the unpaired spin concentration, [S·], remains constant throughout the lightly doped region (Figure 11), then decreases abruptly for $y > 10^{-3}$. Above the semiconductor metal transition, the EPR spectra first became Dysonian (vide supra) followed by disapearance of EPR signal as the line broadens, and the iodine doped polyacetylene becomes a metallic conductor.

Figure 11

C. Iodine doped cis-$(CH)_x$.

EPR saturation curves were also generated from iodine doped cis-$(CH)_x$; the results are shown in Figure 12 and summarized in Table I. In contrast to the results obtained with the trans-isomer, doping of cis-$(CH)_x$ with iodine up to

Figure 12
Table I

$y=3.9 \times 10^{-4}$ does not significantly affect either T_1 or T_2. The signal amplitude decreased as y increased for $y \geq 10^{-3}$ and eventually disappeared near $y=0.03$. The linewidth remained constant throughout the concentration range studied. Another difference between the two polymers is that heavily doped $\underline{cis}$-$(CHI_y)_x$ saturates with pronounced inhomogeneous broadening (Figure 12b) whereas the $\underline{trans}$-materials do not ($\underline{vide}$ $\underline{supra}$).

D. AsF$_5$ doped $\underline{trans}$-(CH)$_x$.

EPR saturation curves were obtained at room temperature for $\underline{trans}$- $[CH(AsF_5)_y]_x$ from $y=3.6 \times 10^{-4}$ to 0.14. A few examples are shown in Figure 13. The relaxation data are summarized in Table II. For the lightly doped materials, $y<10^{-3}$, the T_1 and T_2 values are nearly the same as undoped $\underline{trans}$- $(CH)_x$. They are also similar in their EPR linewidth dependence on H_1, increasing 2- to 3-fold from low to high microwave power; implying that the EPR line remains homogeneously broadened. The values of T_1 and T_2 remain substantially unchanged for $10^{-3}<y<10^{-2}$ at $1.3 \pm 0.6 \times 10^{-5}$ sec and $7.5 \pm 0.6 \times 10^{-8}$ sec. The EPR linewidth increase with microwave power was only about 50% to 70% which is smaller than that for more lightly doped polymers.

Above $y=10^{-2}$ the EPR and its saturation behavior underwent significant changes, indicative of the transitional regime between the dilute semiconducting state and the truly metallic state. We note that the EPR could not be saturated in this important intermediate regime, and that the linewidths are independent of H_1. Finally, in the metallic limit at $y=0.14$, the intense Dysonian resonance

Figure 13

Table II

can be saturated, with apparent values of T_1 and T_2, 1.1 x 10^{-6} sec and 0.11 x 10^{-6} sec, respectively. However, the limitation of skin depth may present a complication in carrying out a detailed analysis.

Although there is considerable scatter in the relative intensities to the lowest concentrations, the susceptibilities remain small. In particular, two samples were prepared with $\underline{y}$=0.03 as an independent cross-check on the results of Ikehata et al.[7] Assuming the typical concentration of [S·] in the undoped samples, i.e. ~300 ppm, the susceptibility of the $\underline{y}$=0.028 and 0.031 samples are χ≈5 x 10^{-8} emu/mole which is extremely small and comparable to those reported earlier[7]. As $\underline{y}$ exceeds 0.04 there was a rapid increase of EPR intensity, which again coincides with the report[7] that the Pauli susceptibility is switched on near $\underline{y}$≈5-7%.

DISCUSSION OF RESULTS

Electrically conducting polymers are of interest to both condensed matter physicists and polymer scientists, and one might expect there exist certain language barriers. In the spirit of our previous short communication[13], we would endeavor to make clear those terms necessary for precise description of the system.

Trans-$(CH)_x$ has a planar zig-zag trans-transoid structure. The molecule has a doubly degenerate ground state as it is unchanged when adjacent C-C bonds are interchanged. The molecule undergoes a commensurate Peierls distortion[3] of index 2 so that the adjacent C-C bonds have unequal length. An analogy is the dynamic Jahn-Teller effect of transition metal complex with doubly degenerate electronic state. If there were no Peierls distortion and all the carbon atoms in the backbone were identical, trans-$(CH)_x$ would be an intrinsic metal. The energy gap which results from bond alternation is small so that the polymer is semiconducting.

Soliton, as it applies to the present subject, has a very precise meaning. It is applied to any topological defects in a molecule such as trans-$(CH)_x$ as represented by

$$\tag{6}$$

where the heavy and light lines represent the short and long bonds, respectively, in a weakly alternating π system S· is a neutral soliton which is

paramagnetic with spin half, and $S^+(S^-)$ are positive (negative) solitons which are diamagnetic with spin zero. Chemists may call them delocalized free radical, carbocation and carbanions. However, the solitons have more specific and limited connotation. They are topological defects where the π-amplitude vanishes; note also that the phase of the π wave function changes at the defect. Furthermore, because of ground state degeneracy, the solitons are free to move up and down the chain as π-density wave, in fact with almost the speed of sound. How these defects arise or the solitons are created will be addressed below.

Let us now turn our attention to cis-$(CH)_x$. It has a nondegenrate ground state. If one designates the ground state to have a cis-transoid configuration, interchange of long and short C-C bonds leads to a trans-cisoid configuration which is higher in energy than the former. This difference in the ground state degeneracy in trans- and cis-$(CH)_x$ is of paramount important to the physicists' treatment of the molecules. If defects are created as above, cf. eqn. 2 of reference 13, they have the same topological features as described above yet because the ground state is non-degenerate the defect cannot propagate as π-density wave. On the other hand, if the generation of defect in cis-$(CH)_x$ is acccompanied by the transformation of a segment of the backbone into the trans-configruation, then the defect behaves as a soliton with a well defined boundary defined by the said seqment.

A. Neutral solitons in undoped trans-$(CH)_x$.

We will postpone the discussion of how neutral solitons are created in trans-$(CH)_x$ to a latter section. But the nature of neutral soliton is such that

there can exist only one S· per <u>trans</u>-(CH)$_x$ molecule. Two S· on the same chain would result in their annihilation[13] unless they are separated by interruption of conjugated backbone such as interchain crosslinks or intramolecular cyclization. It has been found by many laboratories that [S·] in undoped <u>trans</u>-(CH)$_x$ is <u>ca.</u> one S· per 1000-3000 CH. Recently, we found by isotopic labeling[29] that the number average molecular weight for polyacetylene is <u>ca.</u> 22,000. One S· per chain would correspond to an S· per 1700 CH units which is in agreement with this observation.
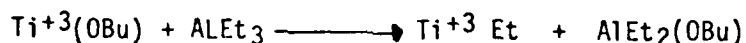
The present results demonstrated that the T_1 of the S· in <u>trans</u>-(CH)$_x$ is decreased even at iodine levels in the range of a few ppm. We assume that the very slow doping technique leads to uniform distribution of the dopant and that the spin-orbit interaction between S· and the dopant is the dominant relaxation mechanism. In this case, in order for the iodine dopant to affect the magnitude of T_1, an S· must diffuse into close proximity of a dopant molecule in a time less than T_1. Using the standard diffusion formula for a random walk in one-dimension

$$\langle x^2 \rangle = 4D_\parallel t \tag{7}$$
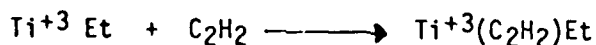
we obtain $D_\parallel \simeq L^2/4T_1$, where L is the mean distance between dopant ions. Since we observe significant reduction in T_1 at levels of the order of 10 ppm, L~10^5 <u>a</u> $= 2 \times 10^{-3}$ cm, where <u>a</u>~1.4 Å is the lattice constant.[17] One estimated $D_\parallel \simeq 5 \times 10^{-2}$ cm^{-2}sec^{-1}. Using the Overhauser effect and analysis of the proton magnetic resonance T_1 data, Nechtschein et al.[30] estimated the longitudinal diffusion constant of <u>ca.</u> 2×10^{-2} cm^{2}sec^{-1}.

The linewidth of the soliton ESR in trans-$(CH)_x$ shows large variation from 0.29 to 2.56G[14,16,31-34]; the T_1 value for undoped trans-$(CH)_x$ also show large scatter (vide supra). Furthermore, the EPR line shape is not purely Lorentzian. Holczer et al.[31] proposed that a small amount of "oxygen localized spins" can dominate the EPR line features of a large majority of highly mobile spins. The effect of short exposure of trans-$(CH)_x$ to oxygen is one of reversible line broadening[14] (vide supra) and reversible p-type doping[35,36]. The permanent consequences of intermolecular crosslinking and intramolecular cyclization after long exposure to oxygen have been discussed previously.[13] The formation of peroxy radicals can also be discounted because the EPR spectra of peroxy radicals with the characteristic g-value[37] was not even detected in readily oxidized polymethylacetylene.[38]

We have considered the possibility of Ti^{+3} contamination from the polymerization catalyst as the source of fixed spins causing significant variability in T_1 and T_2 of trans-$(CH)_x$ and found evidence supporting it. In the polymerization of acetylene, copious quantities of catalyst are used. The $Ti(O-n-Bu)_4$ is reduced by $AlEt_3$ to the active Ti^{+3} species.[15] By analogy to Ziegler-Natta catalyzed olefin polymerizations,[39,40] the initiation process can be written as

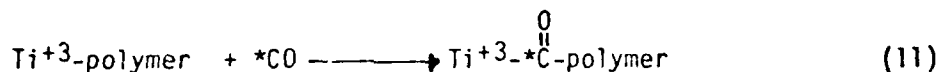$$Ti^{+3}(OBu) + ALEt_3 \longrightarrow Ti^{+3} Et + AlEt_2(OBu)$$

$$(8)$$

$$Ti^{+3} Et + C_2H_2 \longrightarrow Ti^{+3}(C_2H_2)Et$$

the propagation steps as

$$Ti^{+3}(C_2H_2)Et + \underline{n}C_2H_2 \longrightarrow Ti^{+3}(C_2H_2)_{\underline{n}+1}Et \qquad (9)$$

and the chain transfer process as

$$Ti^{+3}(C_2H_2)_{\underline{n}+1}Et + AlEt_3 \longrightarrow Ti^{+3} Et + Et_2Al(C_2H_2)_{\underline{n}+1}Et \qquad (10)$$

That the above mechanism is essentially correct has been established. The number of Ti^{+3}-polymer bonds can be counted by reaction with $*CO$,[29]

$$Ti^{+3}\text{-polymer} + *CO \longrightarrow Ti^{+3}\text{-}*\overset{\overset{\textstyle O}{\|}}{C}\text{-polymer} \qquad (11)$$

Therefore, the Ti^{+3} bound to polyacetylene will remain even after the most exhaustive washing with inert hydrocarbon as is the usual practice. The fluctuating fields produced by the Ti^{+3} can provide an efficient spin-lattice and spin-spin relaxation mechanism for the highly mobile soliton to give the observed variability in T_1 and linewidth. It is to be noted that not every polyacetyelene molecule has a Ti^{+3} bound to it because of the chain transfer process.

$$Ti^{+3}\text{-polymer} + AlEt_3 \longrightarrow Ti^{+3}\text{-Et} + Et_2Al\text{-polymer} \qquad (12)$$
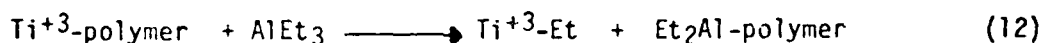
Differential radiotagging experiments[29] had shown that on the average there are four polymer molecules bound to Al to one bound to Ti.

We have analyzed the titanium content (Galbraith Laboratories) in a typical cis-(CH)$_x$ film; it was found to be 0.022 % or 4.6×10^{-6} mole of Ti per gram of polyacetylene. With a number average molecular weight of 22,000 and because only 1/5 of the polyacetylene has a bound Ti due to chain transfer, one expects

9.1×10^{-6} mole of Ti per gram of polymer in good agreement with the analysis. If a typical cis-$(CH)_x$ film is washed under inert atmosphere with 10% HCl in methanol, the Ti content was reduced to 0.011%. Treatment with 30% HCl in methanol gave a Ti content of 0.008%. However, such treatment is unadvisable because the polymer became doped, apparently by HCl as other more effective protonic acids.[41] For instance, cis-$(CH)_x$ washed with 6% HCl in methanol has a conductivity of 2.4×10^{-4} $(\Omega cm)^{-1}$.

We noted that the variability in T_1 of undoped trans-$(CH)_x$ was significantly lowered to ca. ±20% by ppm doping with iodine. This observation is consistent with the above discussion of Ti^{+3} contamination. Iodine acts as an oxidar to convert the paramagnetic Ti^{+3} ion to diamagnetic tetravalent state.

$$Ti^{+3}\text{-polymer} + I_2 \longrightarrow Ti^{+4}I^- + I\text{-polymer} \qquad (13)$$
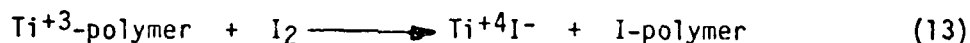
B. Undoped cis-$(CH)_x$

Solitons are not intrinsic to poly(acetylenes); they are induced as neutral defects during isomerization. It has been shown that pristine cis-$(CH)_x$, prepared at low temperature and never exposed to air or warmed up, is devoid of an EPR signal.[15] This implies that the truly pristine polymer is nearly free of structural defects and has predominantly the cis-transoid structure. It was suggested earlier that heating the pristine cis-$(CH)_x$ results in the thermal isomerization of some polymer chain segments to a trans-cisoid configuration with an activation energy of ca. 10 kcal mole^{-1} [16] producing at the same

time a pair of delocalized electrons,

(14)

If the intervening segment is transformed to a trans-transoid configuration

(15)

then the two defects are soliton-antisoliton pair. There is experimental evidence supporting isomerization from cis-transoid to structure 15 directly without the structure 14 as an intermediate. How this transformation which usually requires very high activation energy in olefinic molecules can occur with great ease at very mild conditions is an interesting problem in the understanding of the chemistry of polyacetylene.

Although the soliton-antisoliton pairs in eq. 15 can annihilate one another,

(16)

they can become separated by one or more of the following types of process:

(i) Intramolecular transfer

(17)

(ii) intermolecular annihilation

(18)

(iii) or localized onto Ti at the polyacetylene terminus.

The neutral solitons in partially isomerized cis-$(CH)_x$, which should be more rigorously referred to as cis rich $(CH)_x$, is confined within the segment of trans-transoid structure. Therefore, its EPR is inhomogeneously broadened by unresolved proton hyperfine interaction which can be reduced by substituting deuterium for proton (vide supra). Furthermore, the T_1 and T_2 in cis rich $(CH)_x$ should be less sensitive to the presence of Ti^{+3} impurities; we found this to be true in contrast to the highly variable relaxation times for trans-$(CH)_x$. Finally, iodine doping of cis-rich $(CH)_x$ does not cause detectable changes in relaxation times until y exceeds 10^{-4}.

The proposed mechanism[13] of isomerization implies the existence of a maximum of about one neutral soliton per trans-$(CH)_x$ chain. Our number average molecular weight and [S·] measurements are entirely in agreement with expectation as already stated above.

C. Mechanism of doping.

It was proposed[13] that acceptor doping can take place in trans-$(CH)_x$ via different pathways. The first is the conversion of a neutral soliton directly to a positive spinless soliton S^+,

(19)

Secondly, the acceptor can react with polyacetylene directly to produce a
polaron

(20)

The polaron in <u>trans</u>-$(CH)_x$ is an unstable entity, its fate being dependent upon
whether there exists on the chain a neutral soliton or not. If there is a
neutral soliton they interact to create a S^+,

(21)

If, on the other hand, the chain does not contain a $S\cdot$, then the polaron per-
sists until another polaron is created, the two polarons transform immediately
into a S^+S^+ pair

(22)

Therefore, $S\cdot$ is being depleted slowly and its decrease would be difficult
to detect until the dopant concentration is comparable to the $[S\cdot]$ of one per

trans-(CH)$_x$ chain. Then the decrease in [S·] would become very marked as observed (Fig. 11). Another contributing factor is that when there is present one or more dopants per chain, then a neutral soliton or polaron on one chain can annihilate another one on an adjacent chain via the bridging dopant. In the case of iodine dopant [S·] decreases with $y^{-3.7}$ for $y>10$, which suggests that the dopant exists mainly as I$_3^-$ with I$_5^-$ in minor amounts,[28] in agreement with the conclusions obtained from Raman studies. Moreover, the EPR intensity begins to decrease at $y\sim10^{-3}$, or an I$_3^-$ content of 3 x 10^{-4}, in excellent agreement with the number of neutral solitons in the undoped trans-polymer.

In heavily iodine doped trans-(CHI$_y$)$_x$, the EPR signal becomes Dysonian as the material approaches a metallic state. The EPR signal eventually disappeared, probably resulting from the spin-orbit interaction of the conduction electrons due to overlap of the metallic wave functions onto the I$_3^-$.

The mechanism of doping with AsF$_5$ is similar to that for iodine. The major difference is the much stronger oxidizing power of AsF$_5$. In other words, the direct oxidation of (CH)$_x$ by AsF$_5$ occurs with ease producing polarons (cation radicals) and charged soliton pairs similar to reactions 20-22. Because of this, early EPR studies[14,42] found a general increase of intensity with AsF$_5$ doping which is dependent upon AsF$_5$ pressure. Subsequently, very slow doping procedures were developed in an attempt to optimize homogeneity. With this procedure we found that [S·] remains more or less constant until y exceeds $\sim$3 x 10^{-3} before a significant decrease occured. Earlier measurements[7] demonstrated that for y in the range of a few percent, the absence of a Curie Law set an

upper limit of <1 ppm for [S·]. Thus, all of the neutral [S·] were converted to positively charged soliton, implying a relatively high degree of dopant uniformity.

Doping with AsF_5 at dilute levels has relatively little effect on the relaxation times; the values of T_1 and T_2 for trans-$[CH(AsF_5)_y]_x$ from $3 \times 10^{-4} < y < 6 \times 10^{-3}$ are not significantly different from those of undoped trans-$(CH)_x$, see Table 1. This insensitivity presumably arises from the weaker effective spin-orbit interaction (compared with iodine) and from the small overlap of the neutral solitons onto the $As_2F_{10}^=$ or AsF_6^- species. Similar effects are observed in graphite; intercalation of AsF_5 leads to a narrow, intense EPR signal, whereas after intercalation with iodine the very broad line cannot be detected.

Our inability to saturate the residual EPR of AsF_5 doped samples in the transition region $y \sim 0.03$-0.05 is particularly interesting, and implies values for T_1 less than $\sim 10^{-6}$ sec. The origin of this rapid relaxation in the transitional regime is not presently understood.

CONCLUSION

Pronounced differences were observed between the EPR saturation characteristics of trans-$(CH)_x$ and of cis-$(CH)_x$. They are mostly ascribable to the high mobility of solitons in the trans-isomer and solitons being confined to small domains in the cis-polymer. Iodine in ppm level affects the relaxation behaviors in the former specimens but not in the latter. Analysis of the effect of iodine doping on T_1 leads to an estimate of the spectral soliton diffusion constant in trans-$(CH)_x$, $D_{\parallel} \approx 5 \times 10^{-2}$ cm^2/sec in agreement with values obtained by Nechtschein et al.[30]

REFERENCES AND NOTES

1. This work was supported by a DARPA Contract #N00014-81-K-0648 monitored by the Office of Naval Research.

2. Present address: Materials Science and Engineering Department, Massachusetts Institute of Technology, Cambridge, MA 02139.

3. R.E. Peierls, "Quantum Theory of Solids", Clarendon, Oxford, 1955, p. 108.

4. W.P. Su, J.R. Schrieffer and A.J. Heeger, Phys. Rev. Lett. 42, 1693

5. M.J. Rice, Phys. Letts. 71A, 152 (1979).

6. B.R. Weinberger, J. Kaufer, A.J. Heeger, A. Pron and A.G. MacDiarmid, Phys. Rev. B 20, 223 (1979).

7. S. Ikehata, J. Kaufer, T. Woerner, A. Pron, M.A. Druy, A. Sivak, A.J. Heeger and A.G. MacDiarmid, Phys. Rev. Lett. 45, 1123 (1980).

8. Y.W. Park, A. Denenstein, C.K. Chiang, A.J. Heeger and A.G. MacDiarmid, Solid State Commun. 29, 747 (1979).

9. Y.W. Park, A.J. Heeger, M.A. Druy and A.G. MacDiarmid, J. Chem. Phys. 73, 946 (1980).

10. C.R. Finder, Jr., M. Ozaki, A.J. Heeger, M.A. Druy and A.G. MacDiarmid, Phys. Rev. B 19, 4140 (1979).

11. E.J. Mele and M.J. Rice, Phys. Rev. Lett. 45, 926 (1980).

12. N. Suzuki, M. Ozaki, S. Etemad, A.J. Heeger and A.G. MacDiarmid, Phys. Rev. Lett. 45, 1209 (1980).

13. J.C.W. Chien, J. Polym. Sci., Polym. Lett. Ed. 19, 249 (1981).

14. I.B. Goldberg, H.R. Crowe, P.R. Newman, A.J. Heeger and A.G. MacDiarmid, J. Chem. Phys. 70, 1132 (1979).

15. J.C.W. Chien, F.E. Karasz, G.E. Wnek, A.G. MacDiarmid and A.J. Heeger, J. Polym. Sci., Polym. Lett. Ed. 18, 45 (1979).

16. J.C.W. Chien, F.E. Karasz and G.E. Wnek, Nature 285, 390 (1980).

17. K. Shimamura, F.E. Karasz, J.A. Hirsch and J.C.W. Chien, Makromol. Chem. Rapid Commun., in press.

18. J.C.W. Chien, F.E. Karasz and K. Shimamura, J. Polym. Sci., Polym. Lett. Ed., in press.

19. A.J. Heeger, personal communication.

20. H. Shirakawa and S. Ikeda, Polym. J. 2, 23 (1971).

21. T. Ito, H. Shirakawa and S. Ikeda, J. Polym. Sci., Polym. Chem. Ed. 12, 11 (1974).

22. T. Ito, H. Shirakawa and S. Ikeda, J. Polym. Sci., Polym. Chem. Ed. 13, 1943 (1975).

23. H. Shirakawa, T. Ito and S. Ikeda, Macromol. Chem. 179, 1565 (1978).

24. F.E. Karasz, J.C.W. Chien, R. Galkiewicz, G.E. Wnek, A.J. Heeger and A.G. MacDiarmid, Nature 282, 236 (1979).

25. G.E. Wnek, Ph.D. Dissertation, University of Massachusetts, Amherst, Massachusetts, 1980.

26. J.H. Freed, D.S. Leniart and J.S. Hyde, J. Chem. Phys. 47, 2762 (1967).

27. C.P. Poole and H.A. Farach, "Relaxation in Magnetic Resonance", Academic Press, New York, 1971, Chapters 3,9.

28. S.L. Hsu, A.J. Signorelli, G.P. Pez and R.H. Baughman, J. Chem. Phys. 69, 1 (1978).

29. G.E. Wnek, J. Capistran, J.C.W. Chien, L.C. Dickinson, R. Gable, R. Gooding, K. Gourley, F.E. Karasz, C.P. Lillya and K.-D.Yao, Adv. in Chem., in press.

30. M. Nechtschein, F. Devreux, R.L. Greene, T.C. Clarke and G.B. Street, Phys. Rev. Lett. 44, 356 (1980).

31. K. Holczer, J.P. Boucher, F. Devreux and M. Nechtschein, Phys. Rev. B 23, 1051 (1981).

32. P. Bernier, M. Rolland, C. Linaya and Disi, Polymer 21, 7 (1980).

33. A. Snow, P. Brant, D. Weber and N.L. Yang, J. Polym. Sci., Polym. Lett. Ed. 17, 263 (1979).

34. B. Francois, M. Bernard and J.J. Andre, J. Chem. Phys., in press.

35. J.M. Pochan, H.W. Gibson and F.C. Bailey, J. Polym. Sci., Polym. Lett. Ed. 18, 447 (1980).

36. J.M. Pochan, D.F. Pochan, H. Rommelmann and H.W. Gibson, Macromolecules 14, 110 (1981).

37. J.C.W. Chien and C.R. Boss, J. Am. Chem. Soc. 89, 571 (1967).

38. J.C.W. Chien, G.E. Wnek, F.E. Karasz and J.H. Hirsch, Macromolecules 14, 479 (1981).

39. J.C.W. Chien, J. Am. Chem. Soc. 81, 86 (1959).

40. J.C.W. Chien, J. Polym. Sci. Al 1, 1939 (1963).

41. A.G. MacDiarmid and A.J. Heeger, Synthetic Metals, 1, 101 (1980)

42. Y. Tomkiewicz, T.D. Schultz, H.B. Broom, T.C. Clarke and G.B. Street, Phys. Rev. Lett. 43, 1532 (1979).

TABLE 1

EPR Relaxation Data for cis-$(CHI_y)_x$

y^a	$T_1 \times 10^5$, sec	$T_2 \times 10^8$, sec	ΔH_{pp}, G
3.3×10^{-5}	100	1.1	6.0
4.4×10^{-5}	80	1.0	6.3
7.6×10^{-5}	122	1.0	6.2
1.2×10^{-4}	97	1.0	6.5
3.9×10^{-4}	53	1.0	6.5
3.9×10^{-4}	73	1.0	6.3
1.4×10^{-3}	$--^b$	1.0	6.5-7
4.0×10^{-3}	--	1.0	6.5-7
8.0×10^{-3}	--	1.0	6.5-7
1.3×10^{-2}	--	1.0	6.5-7
2.2×10^{-2}	--	1.0	6.5-7

[a]The first five samples, $y = 3.3 \times 10^{-5}$ to 3.9×10^{-2}, were doped with $^{125}I_2$; the remaining specimens were doped with normal iodine.

[b]No maximum in the saturation curve.

TABLE 2

EPR Saturation Behaviors of Trans-$[CH(AsF_5)_y]_x$

y	Relative EPR intensity	$T_1 \times 10^5$, sec	$T_2 \times 10^8$, sec
3.6×10^{-4}	17	2.5	7.3
1.5×10^{-3}	9.7	1.8	7.3
2×10^{-3}	5.5	1.0	6.6
2.2×10^{-3}	5.3	1.0	8.2
2.5×10^{-3}	17	1.5	7.3
3.7×10^{-3}	9.0	0.8	8.2
6.3×10^{-3}	15.4	1.5	7.3
2.8×10^{-3}	2.5	--[a]	5.0
3.1×10^{-2}	2.6	--	5.5
4.4×10^{-2}	7.0	--	6.9
5.4×10^{-2}	10	--	3.3
0.14	23	0.11	11

[a]EPR cannot be saturated.

(6)

(S·)   (S⁺)   (S⁻)

(13)

A ⇌ B

(14)

B → C

(15)

C →

$$C + A \longrightarrow \text{(16)}$$

$$2C \longrightarrow \text{(17)}$$

$$\text{====} \cdot + I_2 \longrightarrow \underset{\overset{\oplus}{I_3^{\ominus}}}{\text{====}} \quad \text{(18)}$$

$$\cdot \text{====} + I_2 \longrightarrow \underset{\overset{\oplus}{I_3^{\ominus}}}{\text{====}} \quad \text{(19)}$$

$$\underset{\overset{\oplus}{I_3^{\ominus}}}{\text{====}} \cdot \longrightarrow \underset{\overset{\oplus}{I_3^{\ominus}}}{\text{====}} \quad \text{(20)}$$
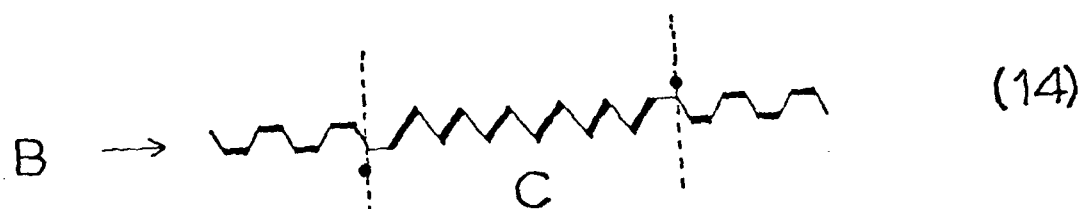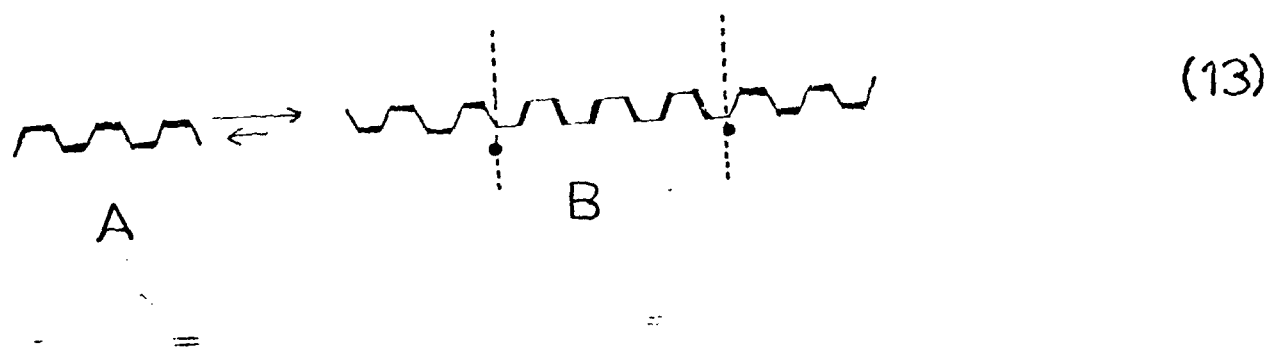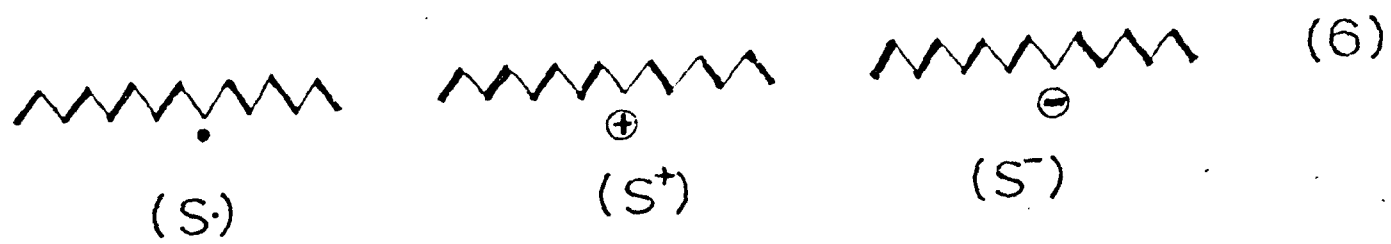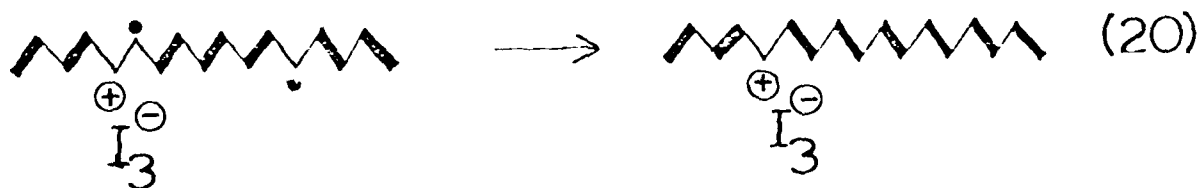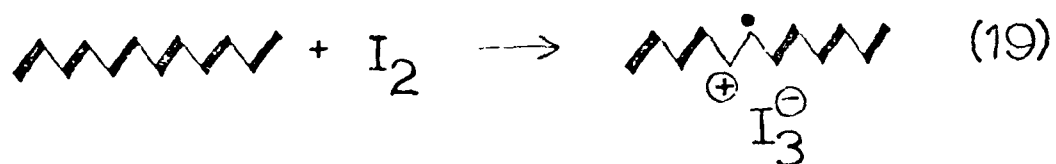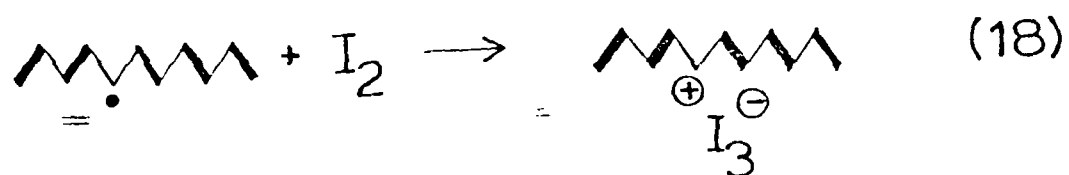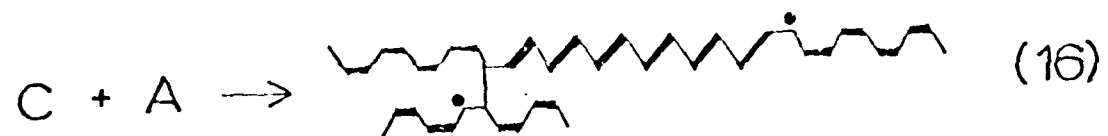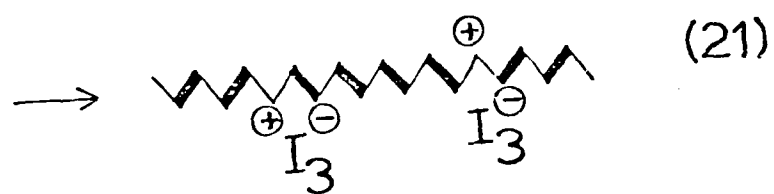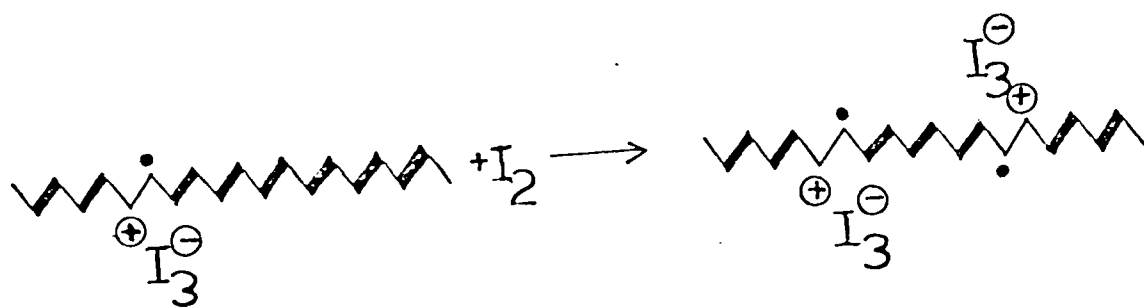
$$\qquad\qquad\qquad\qquad\qquad\qquad\qquad (21)$$

CAPTIONS FOR FIGURES

FIGURE 1:   Variation of conductivity of $\underline{trans}$-$(CHI_y)_x$ with $\underline{y}$.

FIGURE 2:   Plots of specimen temperature as a function of microwave power for $\underline{cis}[CH(AsF_5)_y]_x$: (▲) $\underline{y}=0$; (o) $\underline{y}=5 \times 10^{-3}$; (■) $\underline{y}=8 \times 10^{-3}$; (□) $\underline{y}=1.8 \times 10^{-2}$; ($\triangle$µ $\underline{y}=4.8 \times 10^{-2}$; (o) $\underline{y}=9,4 \times 10^{-2}$.

FIGURE 3:   Electron paramagentic resonance saturation curves at room temperature: (⊖) pristine $\underline{trans}$-$(CH)_x$; (⊡) exposed to air for 15 min; (△) after overnight evacuation.

FIGURE 4:   Electron paramagnetic resonance curves at room temperature: (⊖) cis-$(CH)_x$ sample #1; (△) $\underline{cis}$-$(CH)_x$ sample #2; (□) $\underline{cis}$-$(CH)_x$ sample #3.

FIGURE 5:   Electron paramagnetic resonance saturation curves at room temperature for $\underline{trans}$-$(CHI_y)_x$: (⊖) $\underline{y}=3.8 \times 10^{-6}$; (▲) $\underline{y}=2.0 \times 10^{-5}$; (△) $\underline{y}=5.1 \times 10^{-4}$; (⊡) $\underline{y}=2.5 \times 10^{-3}$; (o) $\underline{y}=1.6 \times 10^{-2}$.
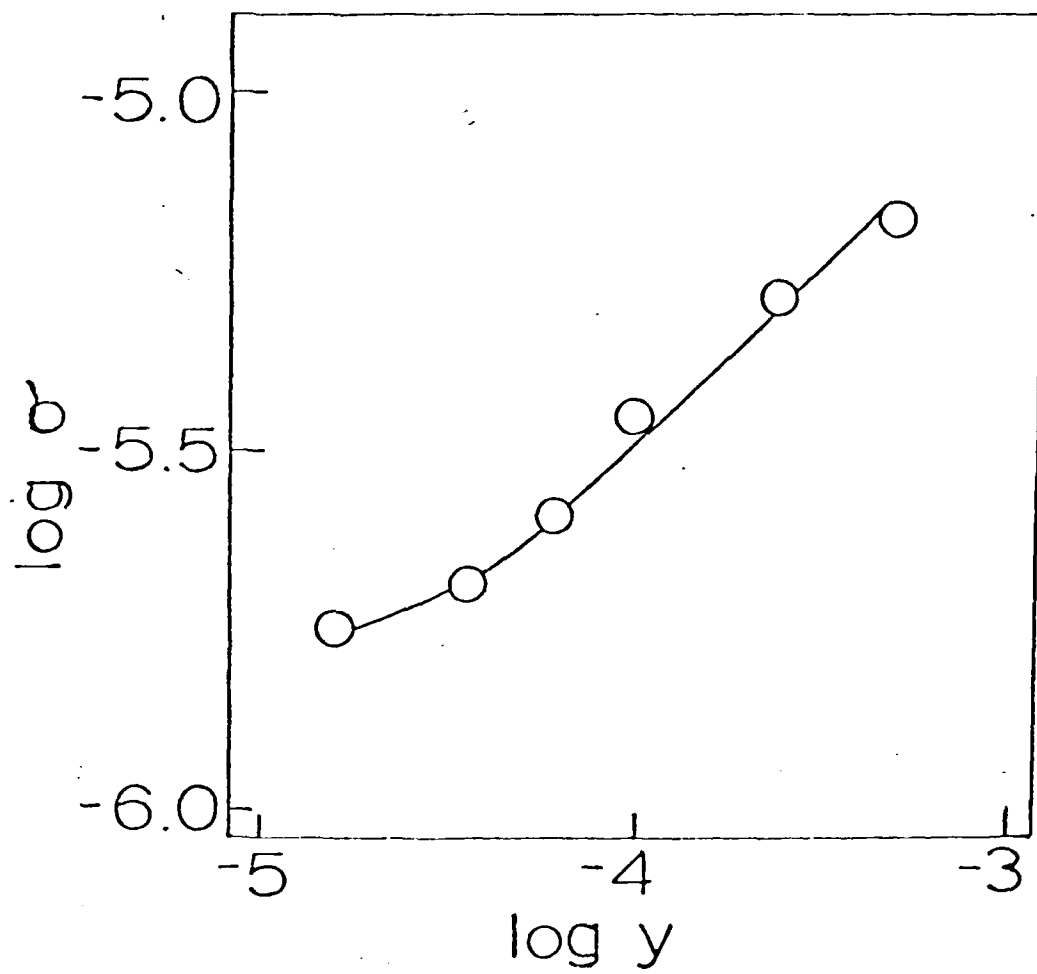
FIGURE 6:   Variation of EPR line width of $\underline{trans}$-$(CH)_x$ with microwave power: (o) at 298°K; (△) at 77°K.

FIGURE 7:   Electron paramagnetic resonance saturation curves at 77°K for $\underline{trans}$-$(CHI_y)_x$: (⊖) $y=7.8 \times 10^{-3}$; (▲) $\underline{y}=1.6 \times 10^{-2}$; (⊡) $\underline{y}=2.2 \times 10^{-2}$.

FIGURE 8:   Variation of T_2 for $\underline{trans}$-$(CHI_y)_x$ with $\underline{y}$.

FIGURE 9:   Variation of T_1 for $\underline{trans}$-$(CHI_y)_x$ with $\underline{y}$.

FIGURE 10: Variation of electron paramagnetic resonance saturation for $\underline{trans}$-$(CHI_{\underline{y}})_{\underline{x}}$.

FIGURE 11: Variation of EPR intensity for $\underline{trans}$-$(CHI_{\underline{y}})_{\underline{x}}$ with $\underline{y}$.

FIGURE 12: Electron paramagnetic resonance saturation curves at room temperature for $\underline{cis}$-$[CHI_{\underline{y}}]_{\underline{x}}$ for (a)(•) $\underline{y}=3.34 \times 10^{-5}$, (△) $\underline{y}=4.4 \times 10^{-5}$, (▣) $\underline{y}=7.58 \times 10^{-5}$, (□) $\underline{y}=1.22 \times 10^{-4}$, (o,▲) $y=3.9 \times 10^{-4}$; (b) (∆) $\underline{y}=1.4 \times 10^{-3}$, (•) $\underline{y}=4 \times 10^{-3}$, (▧) $\underline{y}=8 \times 10^{-3}$, (o) $\underline{y}=1.3 \times 10^{-2}$, (◨) $\underline{y}=2.2 \times 10^{-2}$.

FIGURE 13: Electron paramagnetic resonance saturation curves at room temperature for $\underline{trans}$-$[CH(AsF_5)_{\underline{y}}]_{\underline{x}}$ for: (∆) $\underline{y}=3.6 \times 10^{-4}$; (▨) $\underline{y}=1.5 \times 10^{-3}$; (∆) $\underline{y}=3.7 \times 10^{-3}$; (o) $\underline{y}=2.8 \times 10^{-2}$; (•) $\underline{y}=5.9 \times 10^{-2}$.
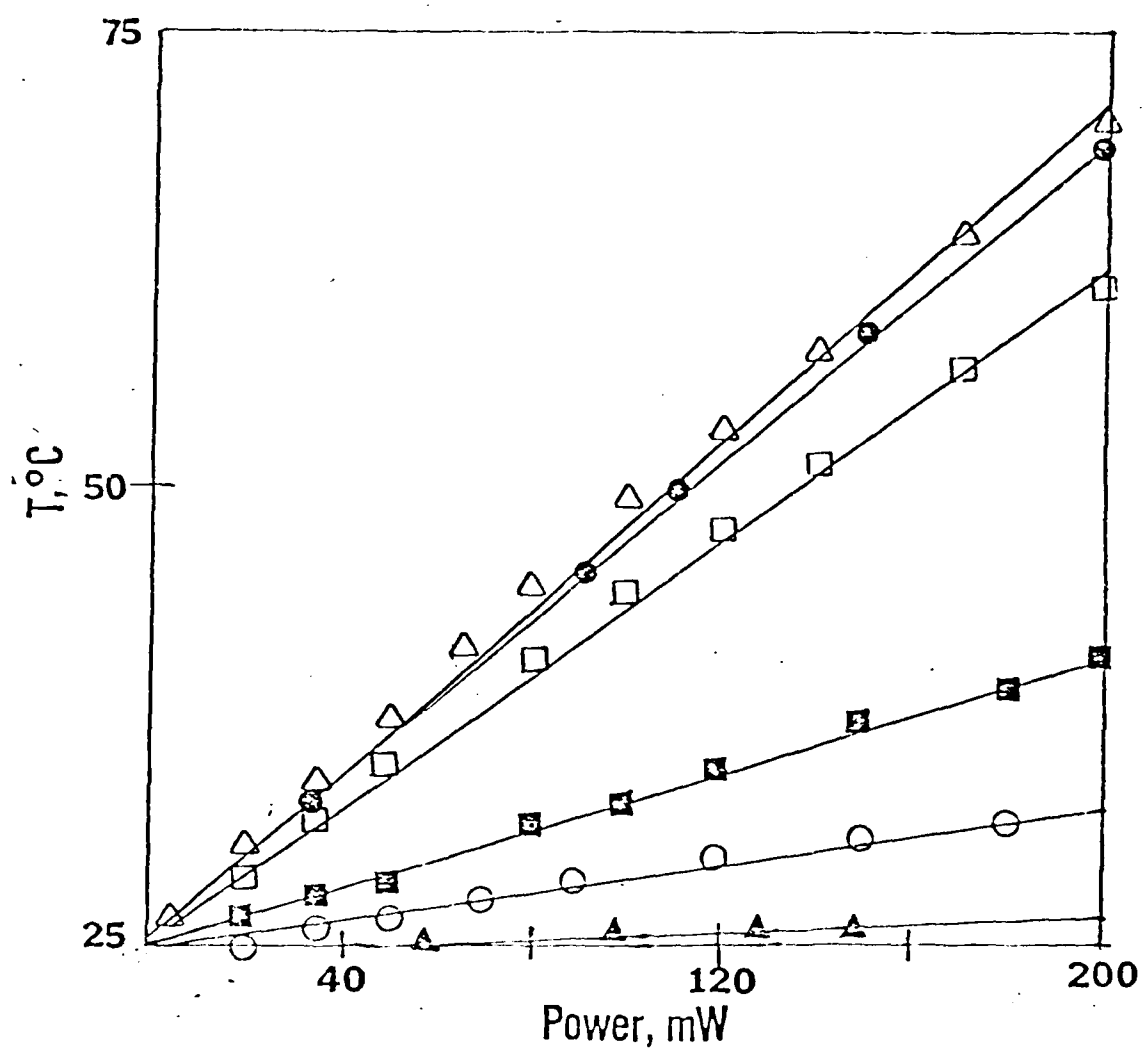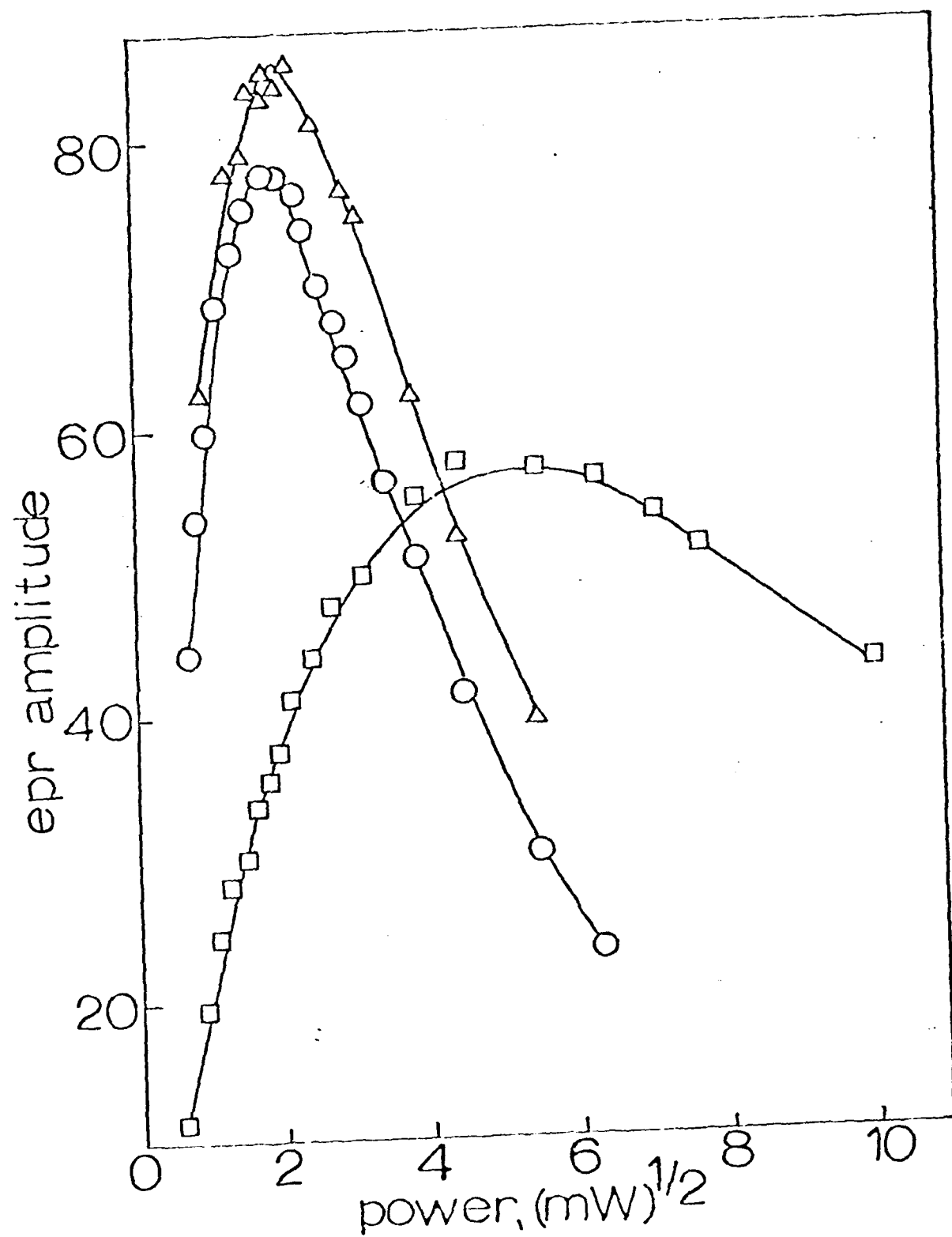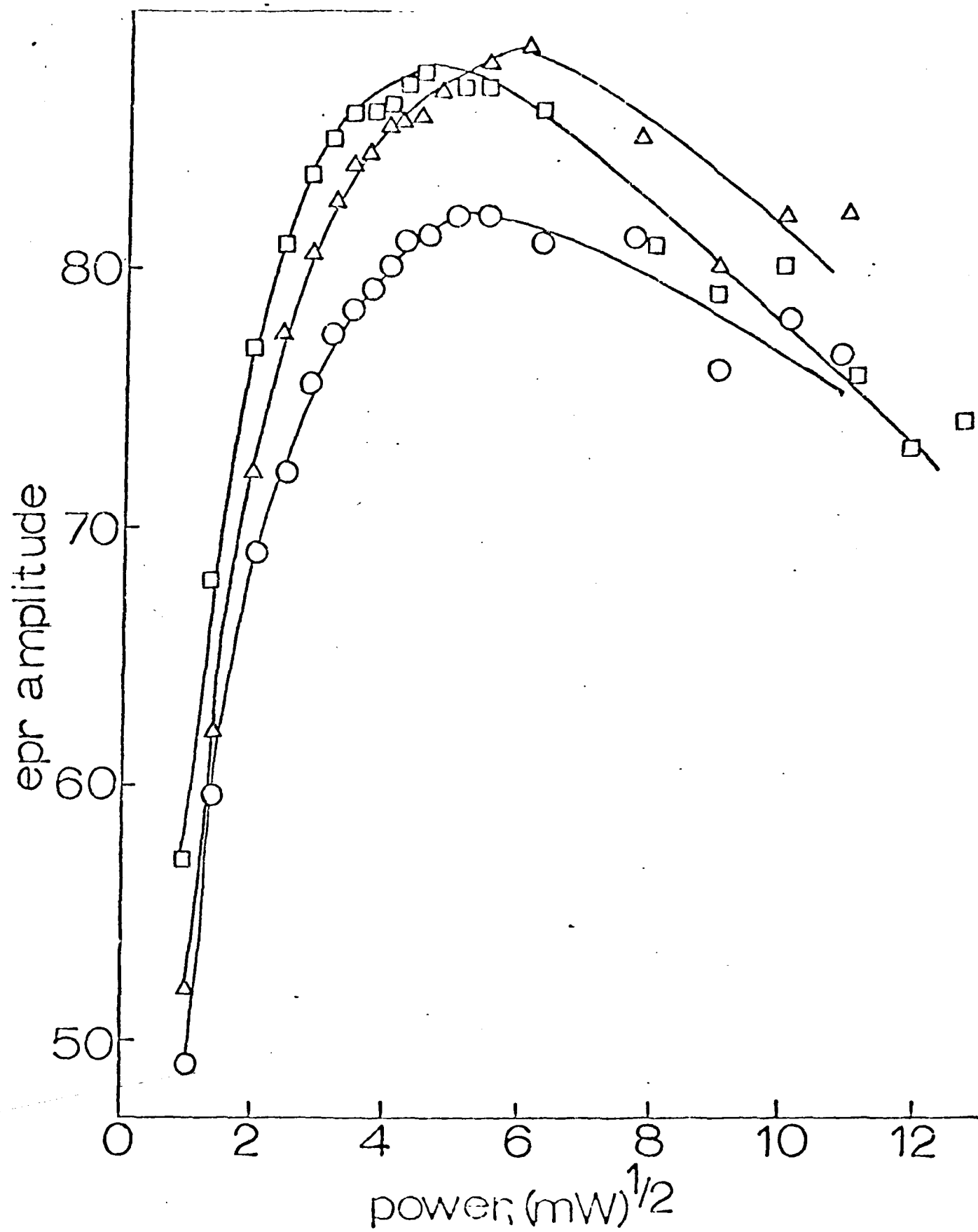
Fig. 1

Fig. 2

Fig. 3

Fig. 4

Fig. 5

Fig. 7

Fig. 8

Axes: vertical axis labeled $T_2 \times 10^9$ seconds (values 40, 50, 60); horizontal axis labeled $-\log y$ (values -2, -3, -4, -5, -6)

Fig.

Fig. 10

Fig. 11

Fig. 12a

The y-axis is labeled "epi amplitude" with values 50, 60, 70 marked. The x-axis is labeled "power, (mW)$^{1/2}$" with values 0, 2, 4, 6, 8, 10, 12 marked.
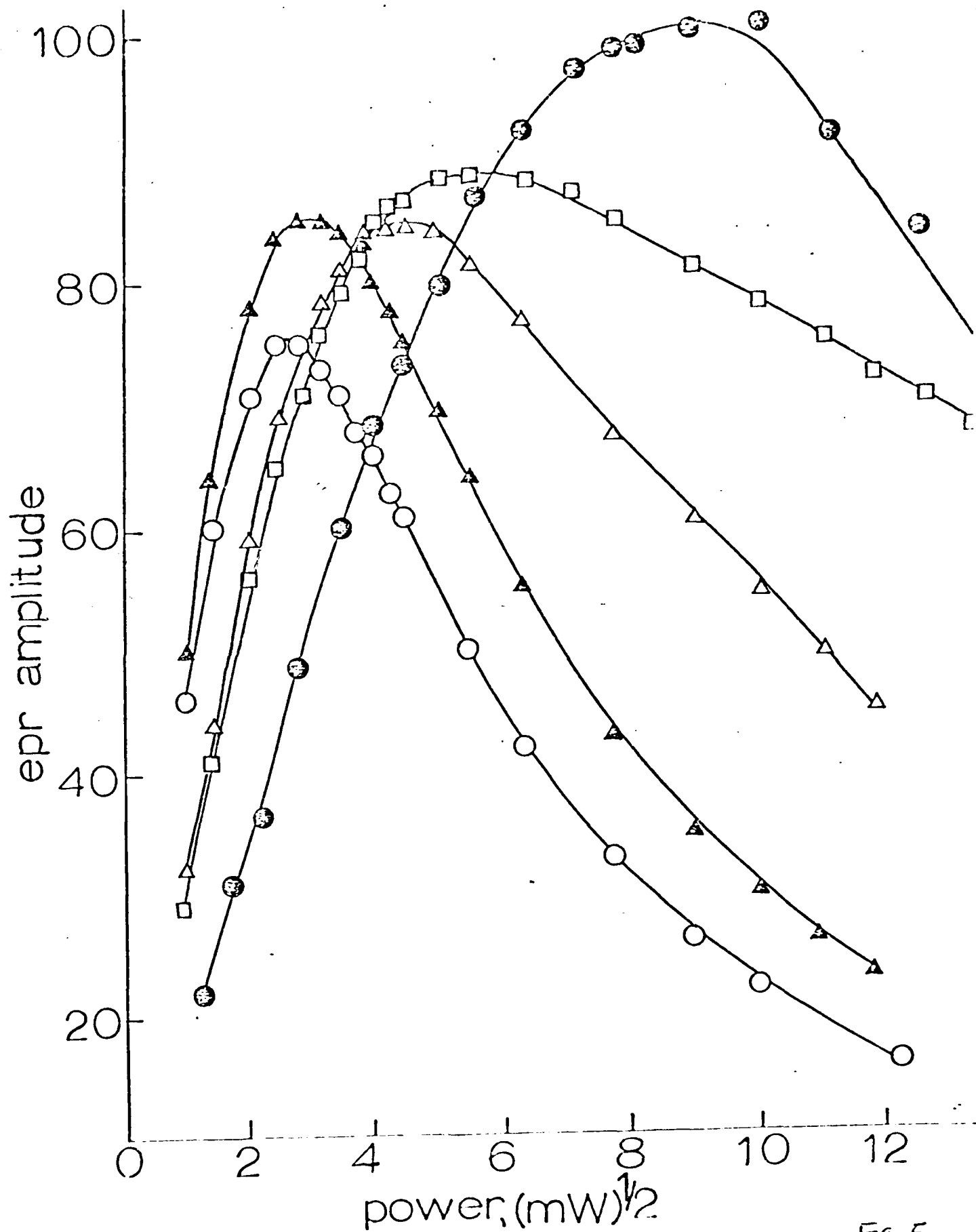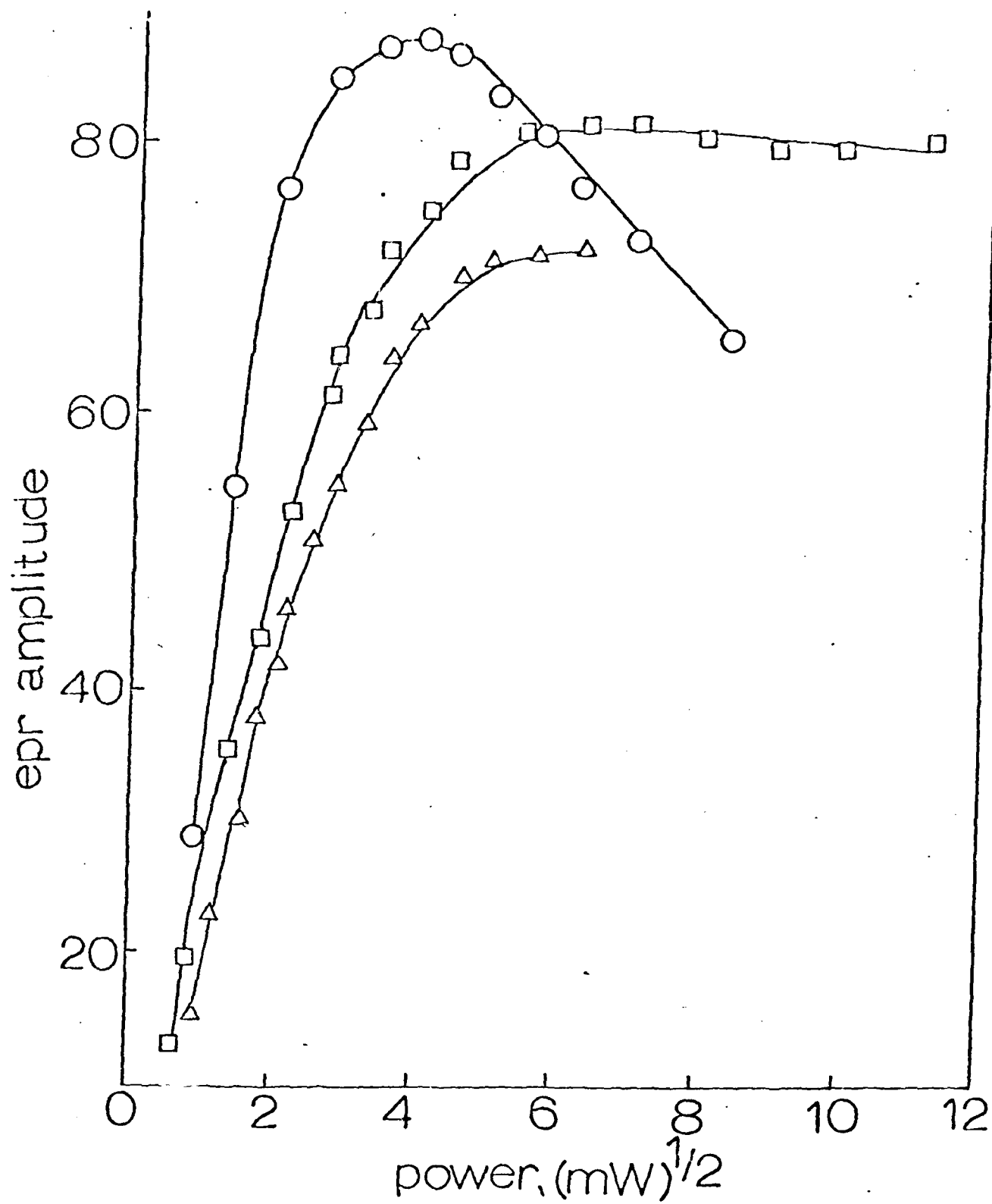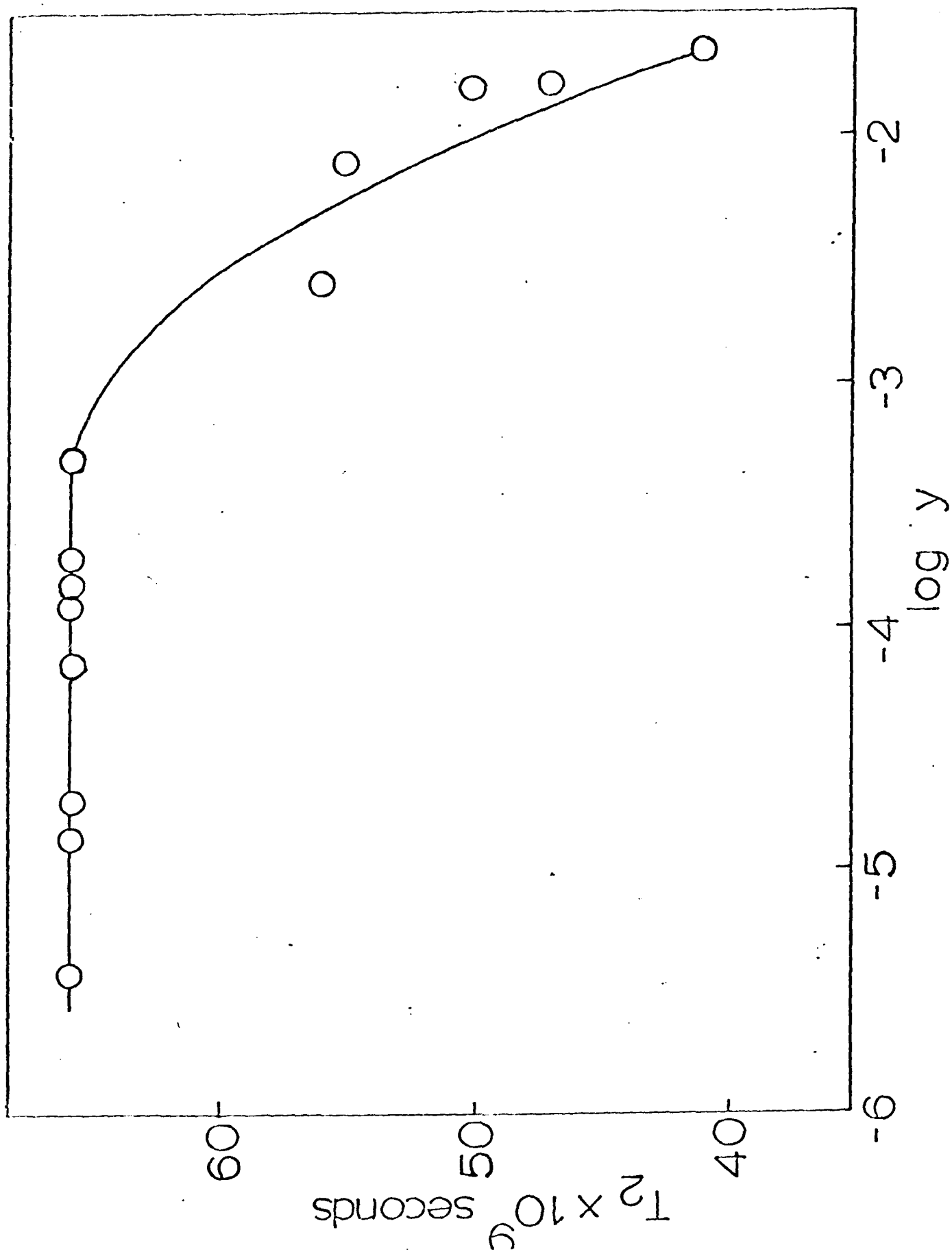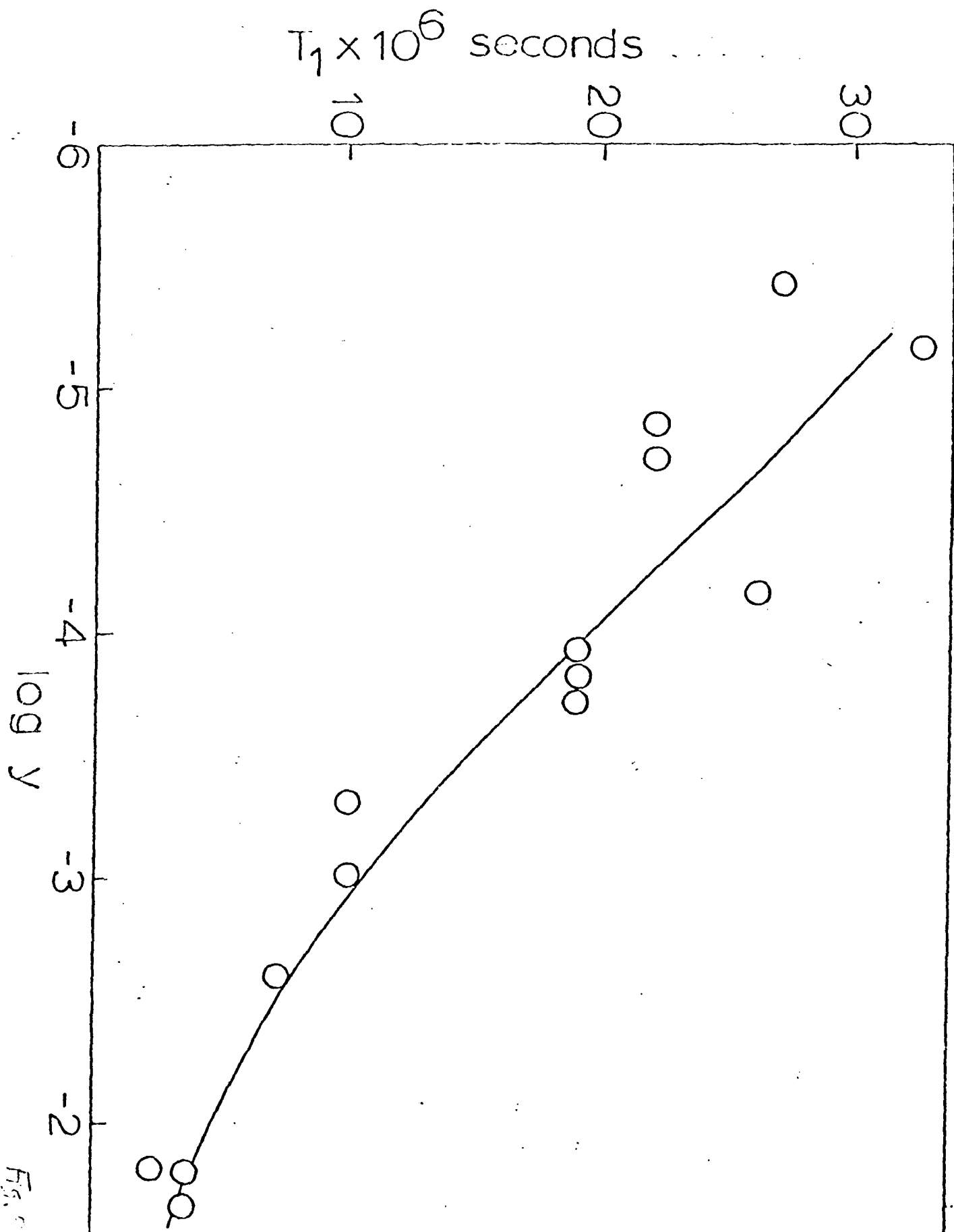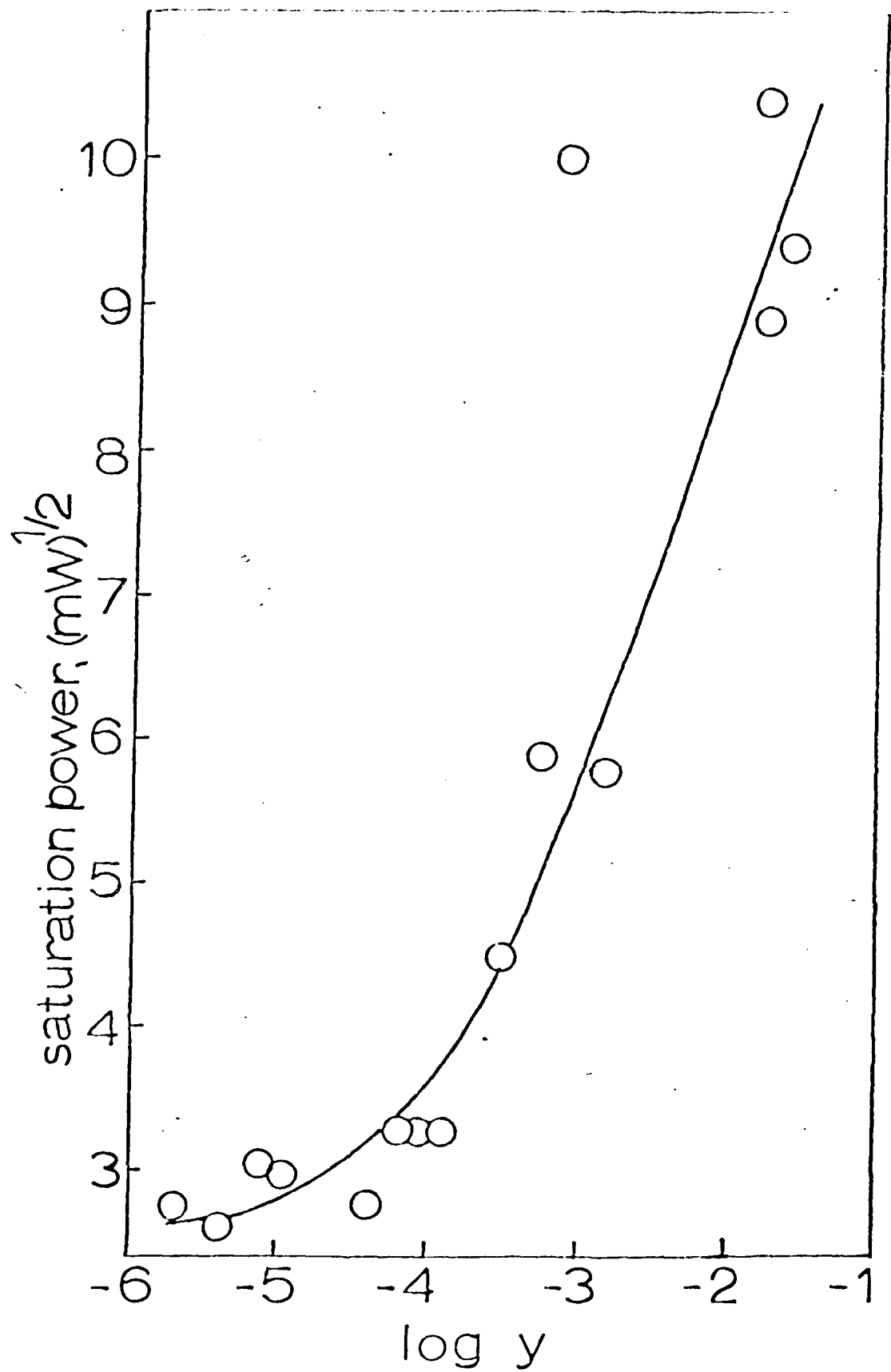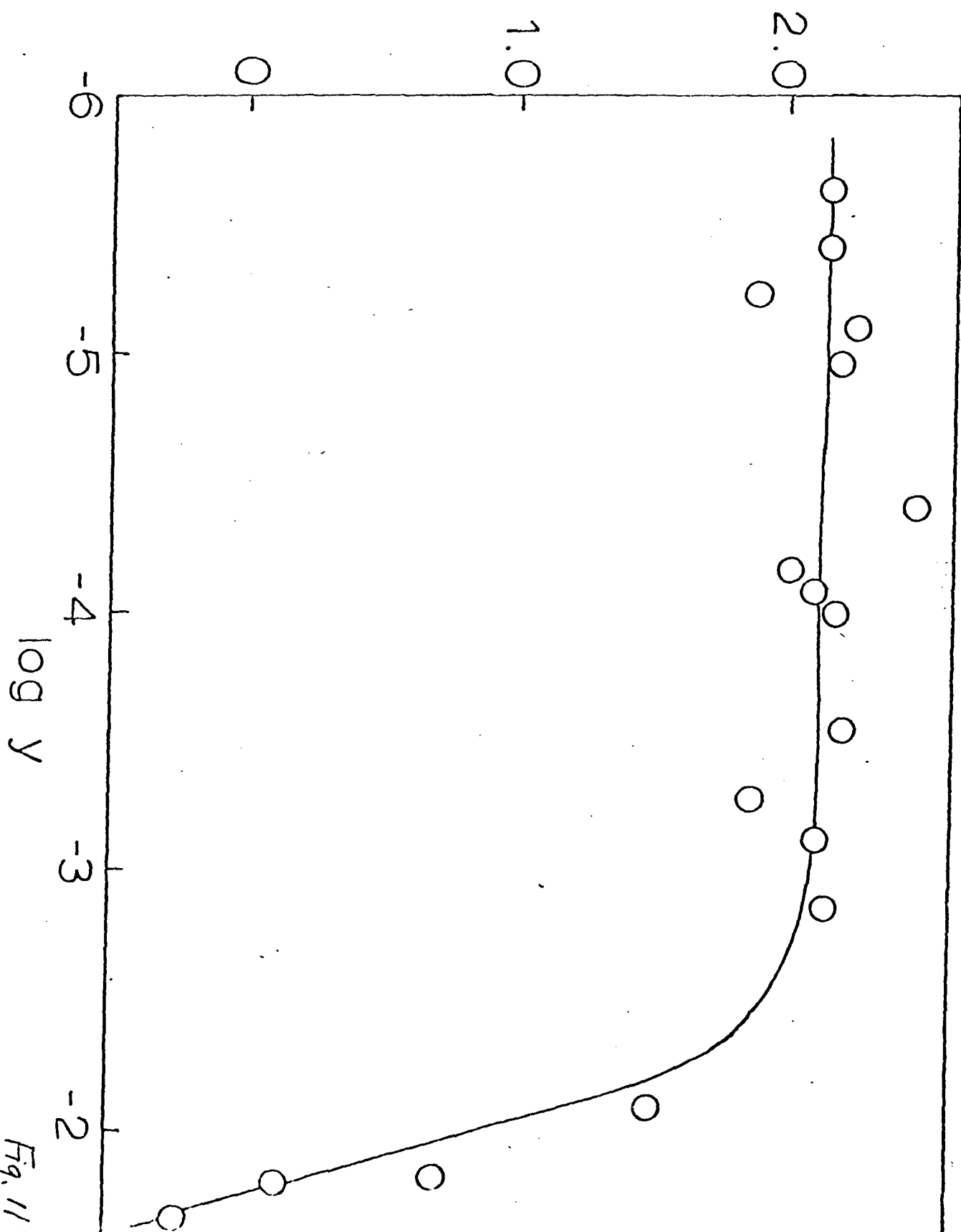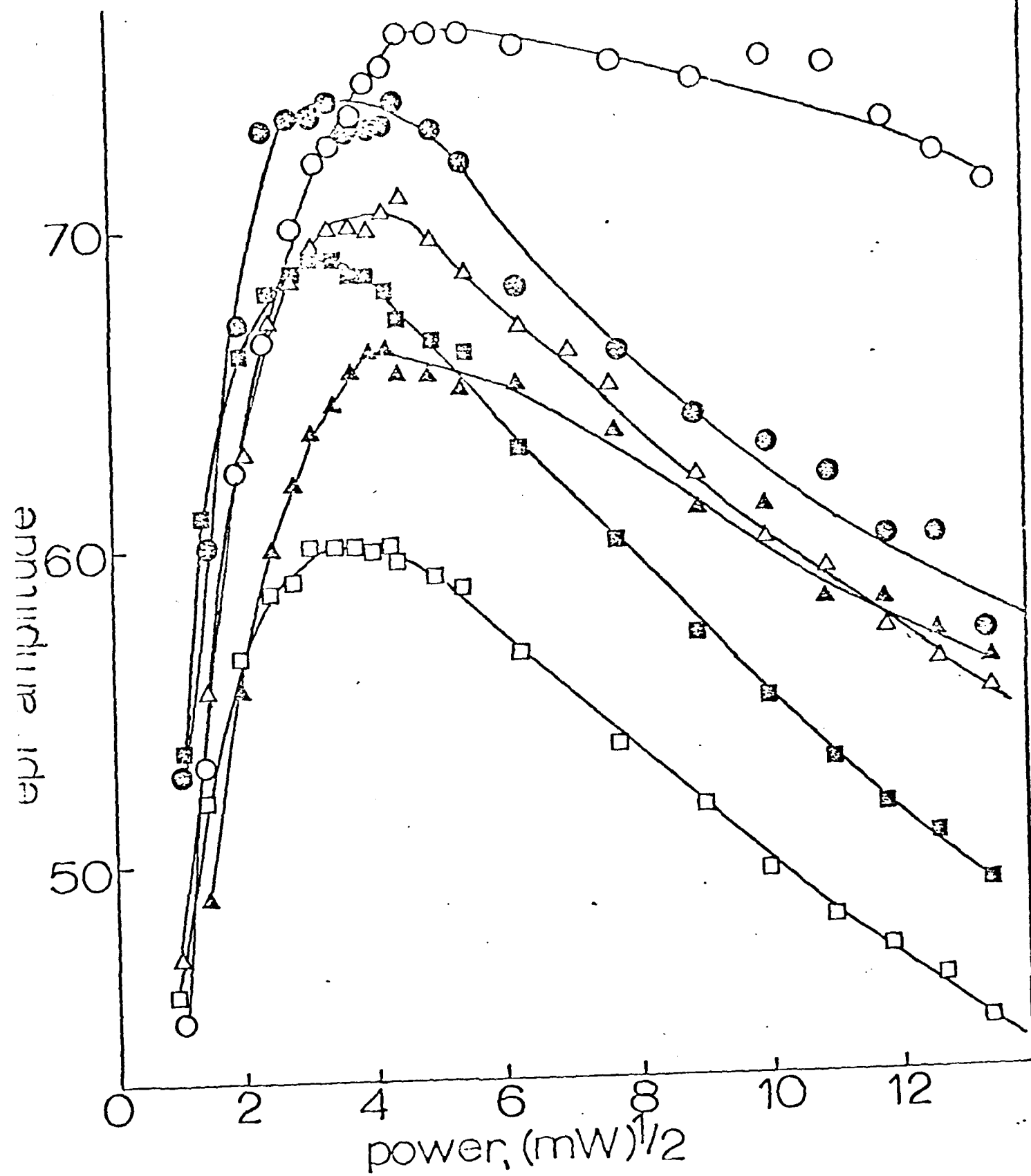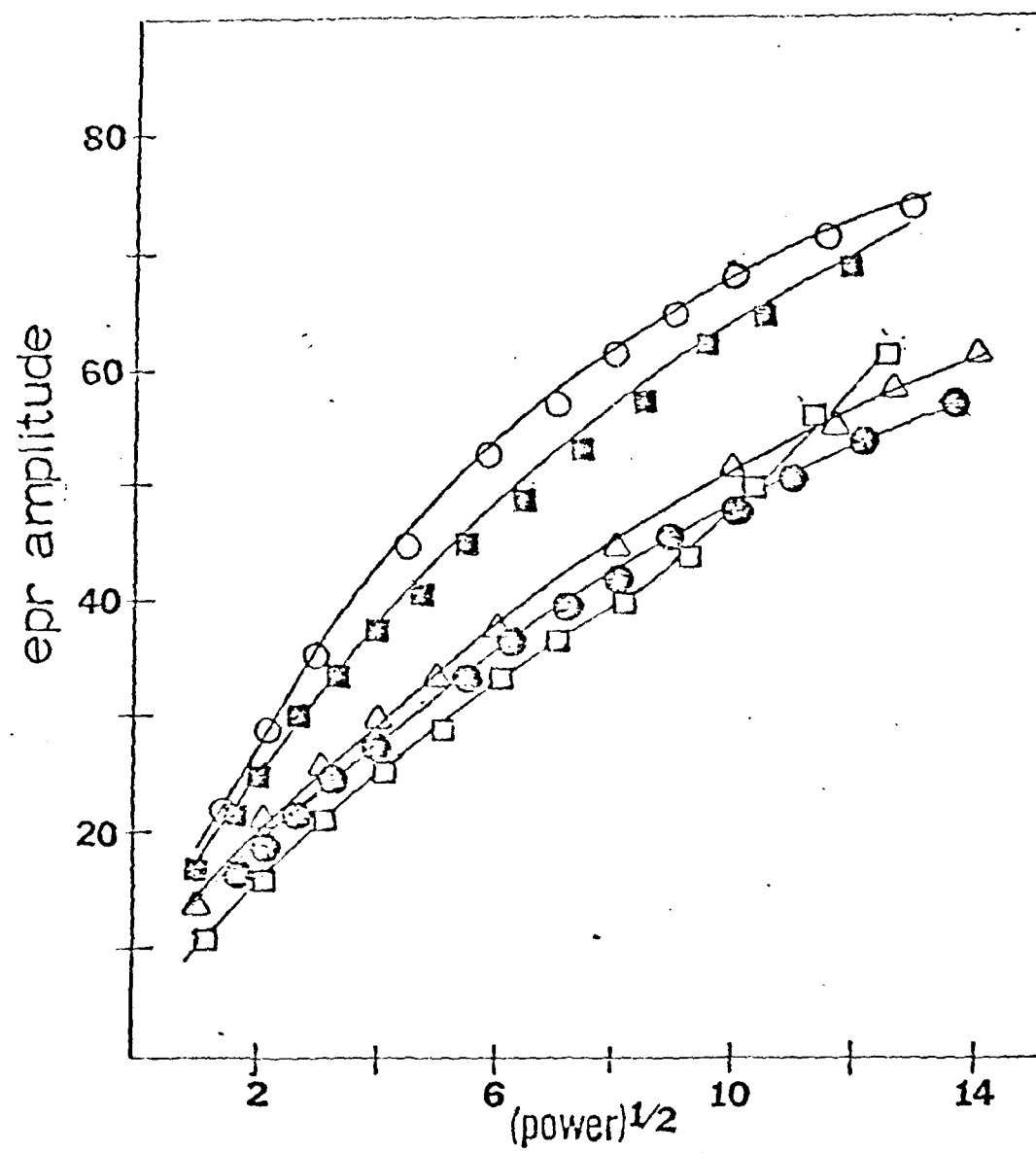
Fig. 12b
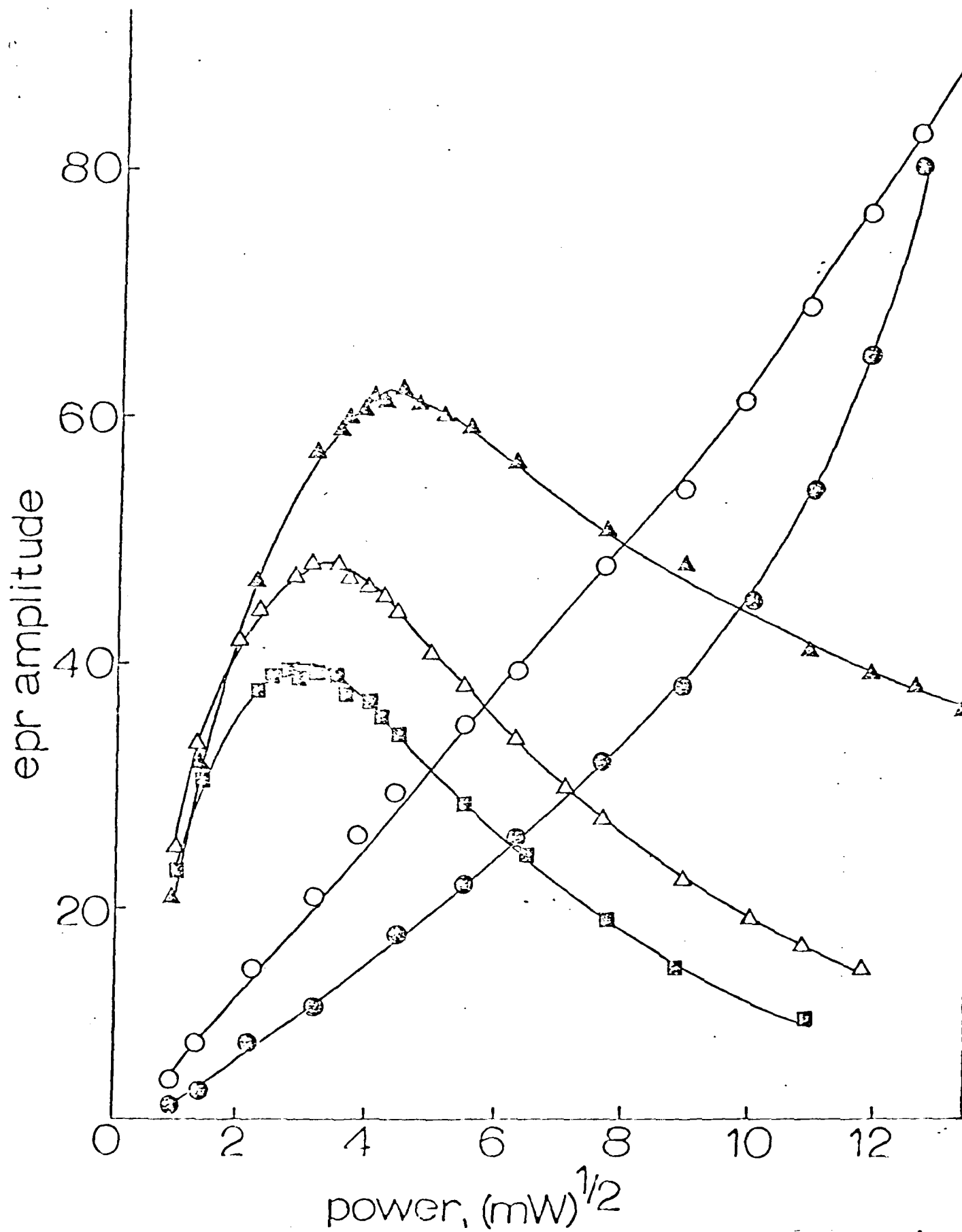
Fig. 13

TECHNICAL REPORT DISTRIBUTION LIST, GEN

	No. Copies		No. Copies
Office of Naval Research Attn: Code 472 800 North Quincy Street Arlington, Virginia 22217	2	U.S. Army Research Office Attn: CRD-AA-IP P.O. Box 1211 Research Triangle Park, N.C. 27709	1
ONR Western Regional Office Attn: Dr. R. J. Marcus 1030 East Green Street Pasadena, California 91106	1	Naval Ocean Systems Center Attn: Mr. Joe McCartney San Diego, California 92152	1
ONR Eastern Regional Office Attn: Dr. L. H. Peebles Building 114, Section D 666 Summer Street Boston, Massachusetts 02210	1	Naval Weapons Center Attn: Dr. A. B. Amster, Chemistry Division China Lake, California 93555	1
Director, Naval Research Laboratory Attn: Code 6100 Washington, D.C. 20390	1	Naval Civil Engineering Laboratory Attn: Dr. R. W. Drisko Port Eueneme, California 93401	1
The Assistant Secretary of the Navy (RE&S) Department of the Navy Room 4E736, Pentagon Washington, D.C. 20350	1	Department of Physics & Chemistry Naval Postgraduate School Monterey, California 93940	1
Commander, Naval Air Systems Command Attn: Code 310C (H. Rosenwasser) Department of the Navy Washington, D.C. 20360	1	Scientific Advisor Commandant of the Marine Corps (Code RD-1) Washington, D.C. 20380	1
		Naval Ship Research and Development Center Attn: Dr. G. Bosmajian, Applied Chemistry Division Annapolis, Maryland 21401	1
Defense Technical Information Center Building 5, Cameron Station Alexandria, Virginia 22314	12		
Dr. Fred Saalfeld Chemistry Division, Code 6100 Naval Research Laboratory Washington, D.C. 20375	1	Naval Ocean Systems Center Attn: Dr. S. Yamamoto, Marine Sciences Division San Diego, California 91232	1
		Mr. John Boyle Materials Branch Naval Ship Engineering Center Philadelphia, Pennsylvania 19112	1

TECHNICAL REPORT DISTRIBUTION LIST, GEN

No.
Copies

Mr. James Kelley
DTNSRDC Code 28?
Annapolis, Maryland 21402   1

Mr. A. M. Anzalone
Administrative Librarian
PLASTEC/ARRADCOM
Bldg 3401
Dover, New Jersey 07801   1

TECHNICAL REPORT DISTRIBUTION LIST, 356B

	No. Copies			No. Copies

Dr. C. L. Shilling
Union Carbide Corporation
Chemical and Plastics
Tarrytown Technical Center
Tarrytown, New York 1

Dr. R. Soulen
Contract Research Department
Pennwalt Corporation
900 First Avenue
King of Prussia, Pennsylvania 19406 1

Dr. A. G. MacDiarmid
University of Pennsylvania
Department of Chemistry
Philadelphia, Pennsylvania 19174 1

Dr. H. Allcock
Pennsylvania State University
Department of Chemistry
University Park, Pennsylvania 16802 1

Dr. M. Kenney
Case-Western University
Department of Chemistry
Cleveland, Ohio 44106 1

Dr. R. Lenz
University of Massachusetts
Department of Chemistry
Amherst, Massachusetts 01002 1

Dr. M. David Curtis
University of Michigan
Department of Chemistry
Ann Arbor, Michigan 48105 1

NASA-Lewis Research Center
Attn: Dr. T. T. Serafini, MS 49-1
21000 Brookpark Road
Cleveland, Ohio 44135 1

Dr. J. Griffith
Naval Research Laboratory
Chemistry Section, Code 6120
Washington, D.C. 20375 1

Dr. G. Goodman
Globe-Union Incorporated
5757 North Green Bay Avenue
Milwaukee, Wisconsin 53201 1

Dr. E. Fischer, Code 2853
Naval Ship Research and
   Development Center
Annapolis Division
Annapolis, Maryland 21402 1

Dr. Martin H. Kaufman, Head
Materials Research Branch (Code 4542)
Naval Weapons Center
China Lake, California 93555 1

Dr. C. Allen
University of Vermont
Department of Chemistry
Burlington, Vermont 05401 1

Professor R. Drago
Department of Chemistry
University of Illinois
Urbana, Illinois 61801 1

COL R. W. Bowles, Code 100M
Office of Naval Research
800 N. Quincy Street
Arlington, Virginia 22217 1

Professor T. Katz
Department of Chemistry
Columbia University
New York, New York 10027 1

Professor James Chien
Department of Chemistry
University of Massachusetts
Amherst, Massachusetts 01002 1

Professor Malcolm B. Polk
Department of Chemistry
Atlanta University
Atlanta, Georgia 30314 1

Dr. G. Bryan Street
IBM Research Laboratory, K32/281
San Jose, California 95193 1